GLO13116

DEVELOPMENT OF DOWNHOLE

GEOTHERMAL HEAT FLUX AND THERMAL

CONDUCTIVITY TRANSDUCERS

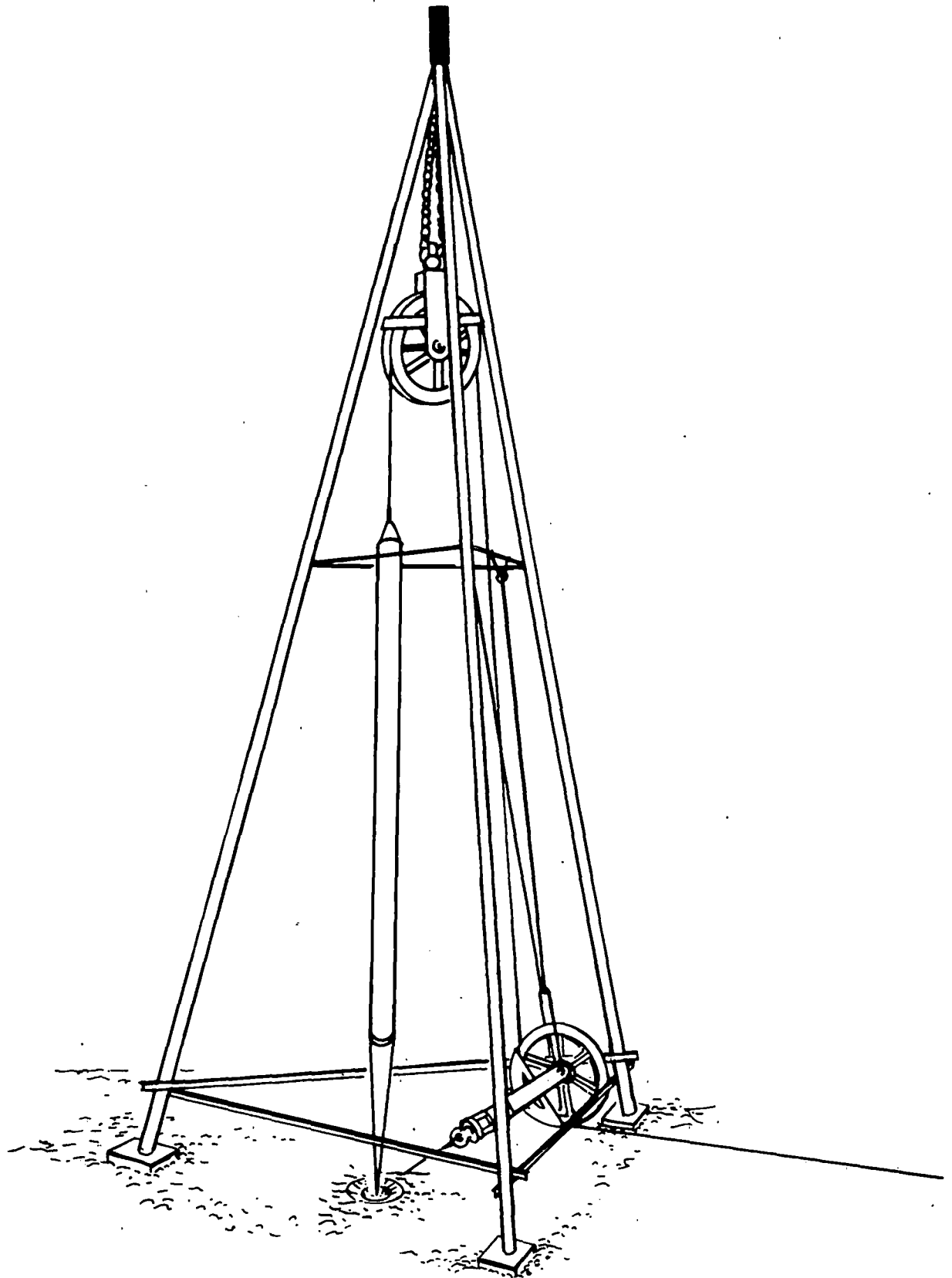For

H. F. Poppendiek
D. J. Connelly
A. J. Sellers
C. M. Sabin
J. G. Dunbar

September 1978

GEOSCIENCE LTD
410 South Cedros Avenue
Solana Beach, California 92075

THE MAST TRIPOD AND A DOWNHOLE TRANSDUCER

TABLE OF CONTENTS

TABLE OF CONTENTS (Continued)

I. INTRODUCTION

Under the present contract from DOE, Geoscience has developed two new transducers which can be used in exploration holes to measure downhole geothermal heat fluxes and earth thermal conductivities. The first step in this effort consisted of analytically describing the performance character-istics of the transducers. Next, models of the transducers were built and tested in the laboratory, verifying the measurement concepts involved. Then a survey was made of possible sites where full-scale transducers could be tested in exploration holes. Consideration was given to open and cased holes, including water-filled and empty holes. It was difficult to find holes that had a diameter of about six inches, were water-filled, had no ground water anomalies, and had normal vertical temperature gradients; the site also had to be accessible. The Phillips Petroleum Company offered Geoscience the use of a test hole near Middletown, California, which was satisfactory. The two transducers were then fabricated and the test plan developed. Next, a joint effort field trip to the test site by Geoscience and Sandia Laboratories was made.[*] Sandia supplied the logging equipment which was needed to lower and raise the Geoscience transducers in the well; Sandia, together with Gearhart-Owen, also made caliper and temperature measurements prior to the transducer tests.

---

[*] Sandia is the technical governmental monitoring group for the Geoscience DOE contract.

Although this report outlines some technical background material for the two transducers, it primarily describes (1) the transducer field test effort at Middletown, (2) the downhole measurements made, and (3) the geothermal heat flux and thermal conductivity data derived from the transducer measurements. The results obtained by the two transducers are compared to each other and to other pertinent data.

II. DESCRIPTION OF THE MEASUREMENT TECHNIQUES

The objective of this program has been to develop methods of measuring directly the geothermal heat flux and the thermal conductivity of the surrounding earth in exploration wells. The rod heat flux transducer and the thermal conductivity probe conceived by Geoscience are two different sensor systems that can measure these two important parameters.

Prior to the development of the two transducers described in this document, the primary method of determining the thermal conductivity of the earth surrounding a well was to remove cores or drill chips for measurement in a laboratory. From in-place vertical temperature gradient measurements and the laboratory thermal conductivity measurement, the vertical heat flux was determined. The conductivity measurement is generally made in what is called a "divided bar apparatus," which involves the comparison of the rock sample with a specimen whose thermal conductivity is known. This method has a number of disadvantages. One is the difficulty in acquiring samples for measurement, which in many cases is not economical. Also, the time required to determine the thermal conductivity can be excessive. Further, only relatively solid rock samples can be used since the divided bar method requires that high pressures (about 2000 psi) be applied to the sample in order to reduce contact resistance. The water content of the rock sample may also vary during the collection and transportation processes, due to evaporation, which may affect the measured thermal conductivity.[1] There are more accurate methods of measuring the thermal conductivity of rocks

than the divided bar method;[2] however, most of the disadvantages listed above still apply.

A. Rod Heat Flux Transducers

Consider the idealized rod heat flux transducer system shown in Figure 1. A steady state heat transfer analysis of this boundary value problem has been made which relates all of the system parameters[3] (see the Appendix for the analytical closed form functions). The solution contains two unknowns, namely, the thermal conductivity of the earth and the vertical earth temperature gradient. These two unknowns can be evaluated by making steady state thermopile voltage measurements with two rod transducers of different but known thermal conductivities. The model also accounts for the effect of a fluid annulus between the transducer and the borehole wall on the temperature field.

The equations for the temperature distribution along the rod heat flux transducers are functions only of the thermal conductivity of the earth, the temperature gradient, and the physical characteristics of the transducers. If the known physical constants for each of the two transducers are substituted into the equations, the resulting equation for one transducer can be divided by the equation for the other transducer. This ratio is then only a function of the earth thermal conductivity because the temperature gradient in the earth cancels out; Figure 2 gives a graph of such a generalized function. Specifically, the earth conductivity is plotted versus the ratio of the thermopile temperature differences (or voltage differences) for the two rod transducers used at Middletown. Note that the radius of influence, r_o, is not a sensitive parameter.
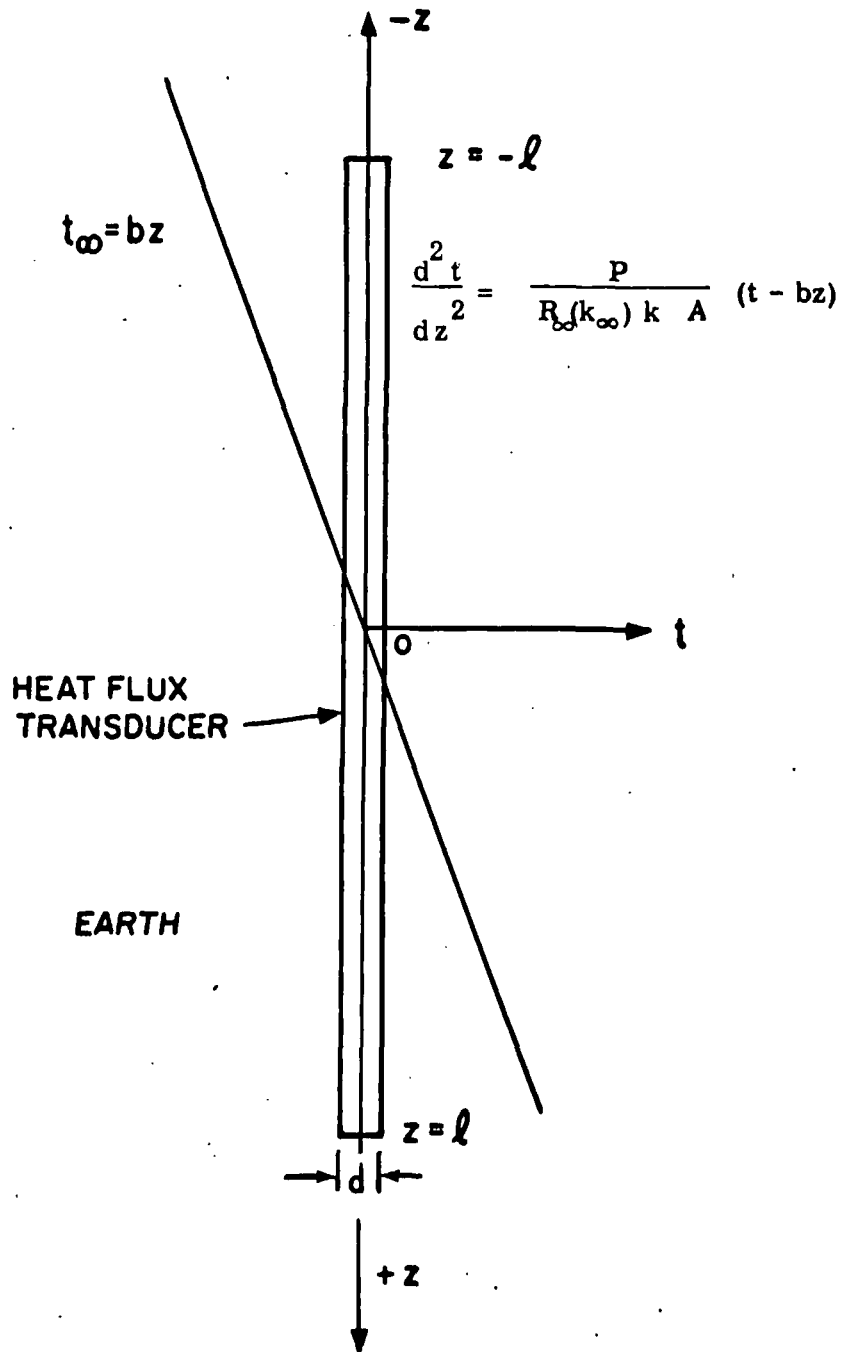
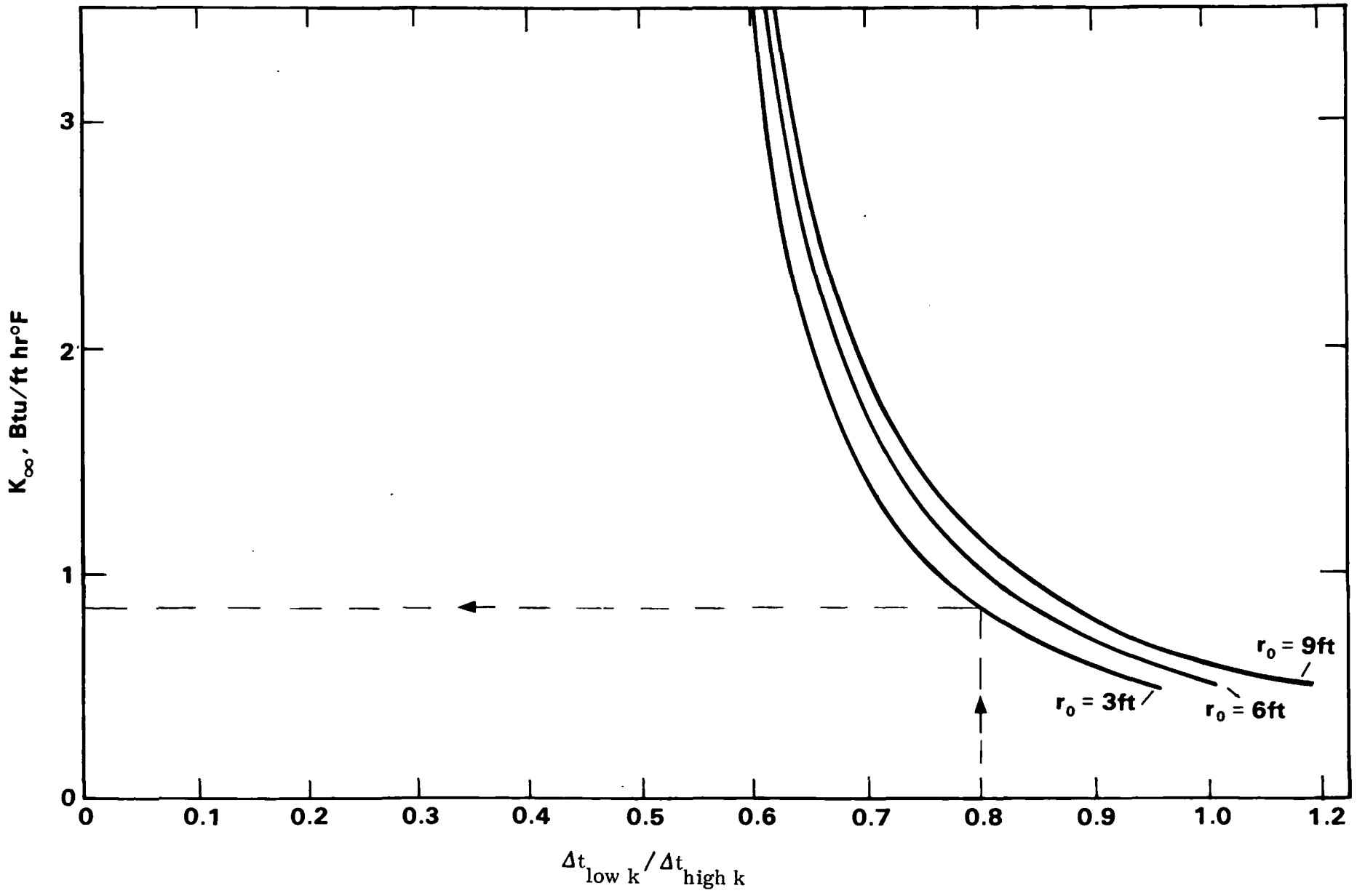Figure 1. Idealized thin rod transducer system

Figure 2. k_∞ versus $\Delta t_{low\ k} / \Delta t_{high\ k}$ and r_o.

An example of the thermal conductivity determination is shown in
Figure 2. If the Δt ratio (or the output voltage ratio) is 0.8, the thermal
conductivity of the rock is read from the graph as 0.85 Btu/ft hr °F at an
r_o value of three feet. Next, the voltage output of the low conductivity
rod transducer thermopile is converted to a temperature difference and
this quantity is divided by the known length of the thermopile in this trans-
ducer to obtain the local temperature gradient. This gradient is then
multiplied by the measured thermal conductivity to determine the geothermal
heat flux. For example, if the temperature gradient were 0.04°F/ft,
the heat flux (for the illustrative thermal conductivity noted above) would
be 0.034 Btu/hr ft^2 (2.6 μ cal/sec cm^2).

B. Thermal Conductivity Probe

Consider the idealized cylindrical thermal conductivity probe system
shown in Figure 3. Mathematical heat transfer models have been used
to relate the earth thermal conductivities (and the thermal capacities
per unit volume) to the time-temperature measurements, the electrical
surface heat addition and the system geometry. Also included in the
models is the effect of a fluid annulus between the probe and the borehole
wall on the temperature field. The analytical functions for the model
are given in the Appendix.[4,5]

The downhole measurements can be made with a thermal conductivity
probe which consists of a long cylindrical section containing a surface
heater and a thermopile that measures the temperature rise of the heated
surface above a reference temperature. A time versus temperature
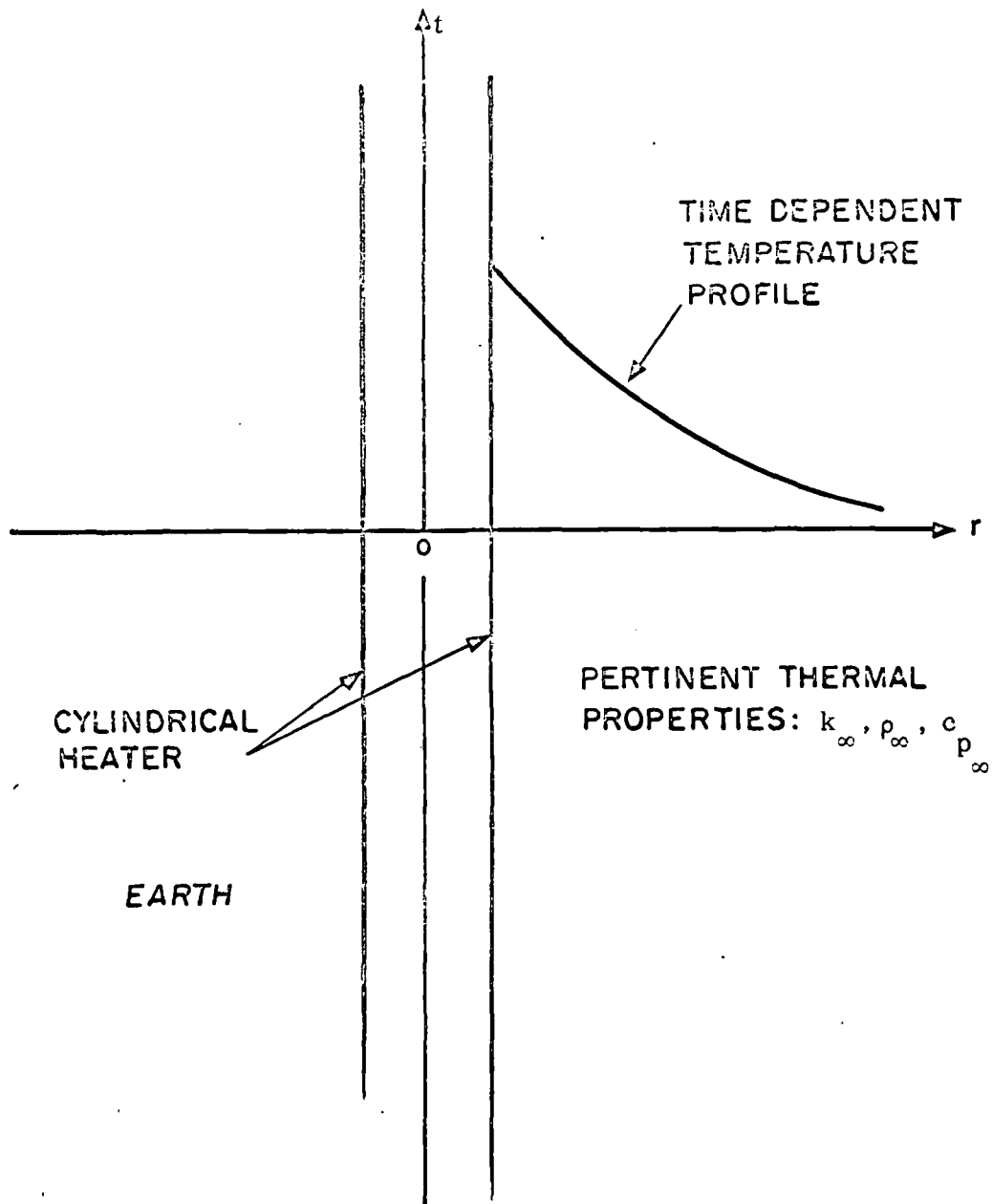recording is made while power is applied to the transducer heater and

Figure 3. Cylindrical thermal conductivity probe system.

the trace is then compared to a number of previously-calculated curves which cover a range of thermal conductivity and heat capacity per unit volume values. At short time periods after the beginning of the constant heating process, the thermal capacity per unit volume has a more pronounced effect on the time-temperature function than does the thermal conductivity. For longer time periods after heating initiation, the thermal conductivity is more important. The curve which matches the recording most closely is then used to obtain the thermal conductivity. An example of such a curve is given in Figure 4. The process of determining the geothermal heat flux is the same as that outlined for the rod heat flux transducer.

C. Advantages of the New Downhole Measurement Techniques

Geoscience has reviewed the literature on the methods being used by the geothermal community to assess geothermal reserves. Included are the geochemical, magnetic, electrical resistivity, microseismic, acoustic, infrared imagery, and the heat flux methods.[6] Discussions have also been held with technical staff members of geothermal exploration companies and the U. S. Geological Survey. Generally, workers involved with thermal techniques feel that heat flux is a logical and appropriate index of the strength of the geothermal reserve; Geoscience also supports this view. For example, from an integration of the measured heat flux over a geothermal reserve and consideration of information on the lithology, quantitative estimates on the reserve strength can be made.
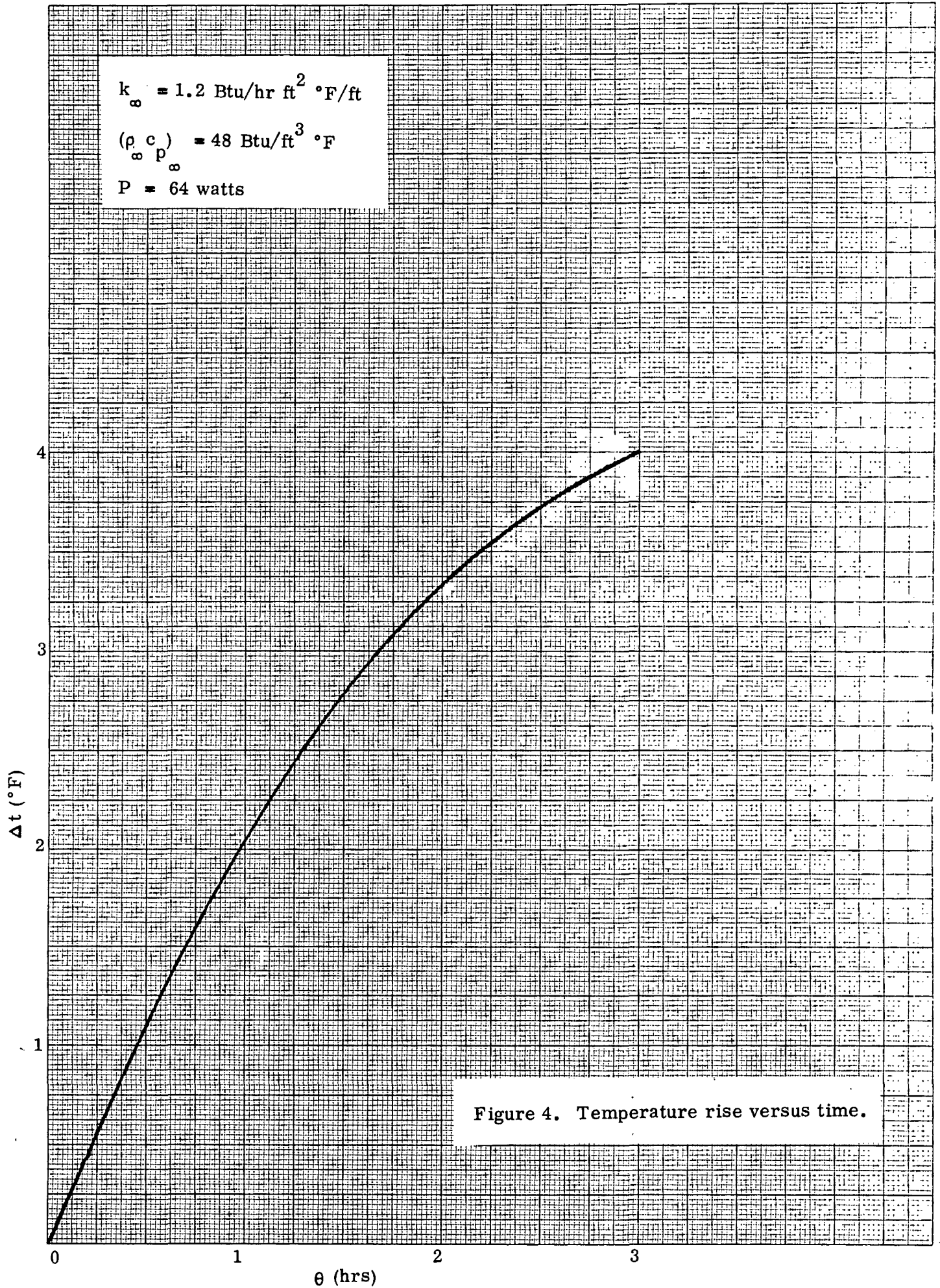
Figure 4. Temperature rise versus time.

Clearly, the in-situ measurement of thermal conductivity and heat flux using the two transducers presented here has several advantages. The number of steps required to determine these parameters are fewer than those required by the current methodology and the time required to make a measurement is much shorter.

It is possible to make an approximate, comparative cost evaluation for the new transducers (relative to the current technology). In the case of the current technology, three major steps are required, namely, (1) the obtaining of core samples as a function of depth, (2) well temperature logging, and (3) thermal conductivity measurement of the core samples. In the case of the new technology (using either the rod heat flux transducer or the thermal conductivity probe), only one major step is required, namely, measuring temperature gradients (with respect to distance or time). As a first approximation, it is estimated that the cost of each of the steps listed for the current and new measurement techniques is the same. On this basis, the cost of the new technology would be about one-third the cost of the old technology. Because of the relatively long lifetimes of the equipment associated with both the current and new methods, the prorated capital cost is small. Further, the capital cost for the two Geoscience transducers is not great (of the order of one to two thousand dollars per transducer).

III. DESCRIPTION OF THE TRANSDUCERS

The structure of the rod heat flux transducer is rather simple. It consists
of a thick wall aluminum cylinder that houses an internal fifty-junction-set
thermopile. The thermopile is electrically insulated from the rod and is
sealed by means of two end plates having O-rings. One end plate contains
a seven-conductor Gearhart-Owen connector. Vermiculite insulation is packed
into the central hole so that there is no relative motion of the thermocouple
wires. A schematic drawing of the two main components of the rod heat flux
transducer is noted in Figure 5. Figure 6 shows a photograph of the end view
of the thick wall aluminum cylinder with the thermopile and end clamp in
place, prior to adding the vermiculite; the end plate with an O-ring is also
shown in this view. When Teflon O-rings are used in this system, the trans-
ducer can operate in temperature fields up to 550°F. The working drawings
for this transducer have been presented previously.[7]

The structure of the thermal conductivity probe is more complex than that
of the rod heat flux transducer. The former transducer consists of (1) a thin
wall stainless steel shell, (2) a surface thermopile, (3) a surface heater,
(4) a large volume of vermiculite insulation, and (5) end plates. A schematic
drawing of the main components of the thermal conductivity probe is shown
in Figure 7. The thermopile and surface heater circuits are electrically
insulated from each other by thin Teflon sheets. The thermopile-heater matrix
is pressed against the stainless steel shell by many low-mass, high-pressure
clamps. After the thermopile and heater leads were attached to the Gearhart-
Owen connector and the end plate was welded into position, vermiculite was

OUTPUT LEADS TO SURFACE
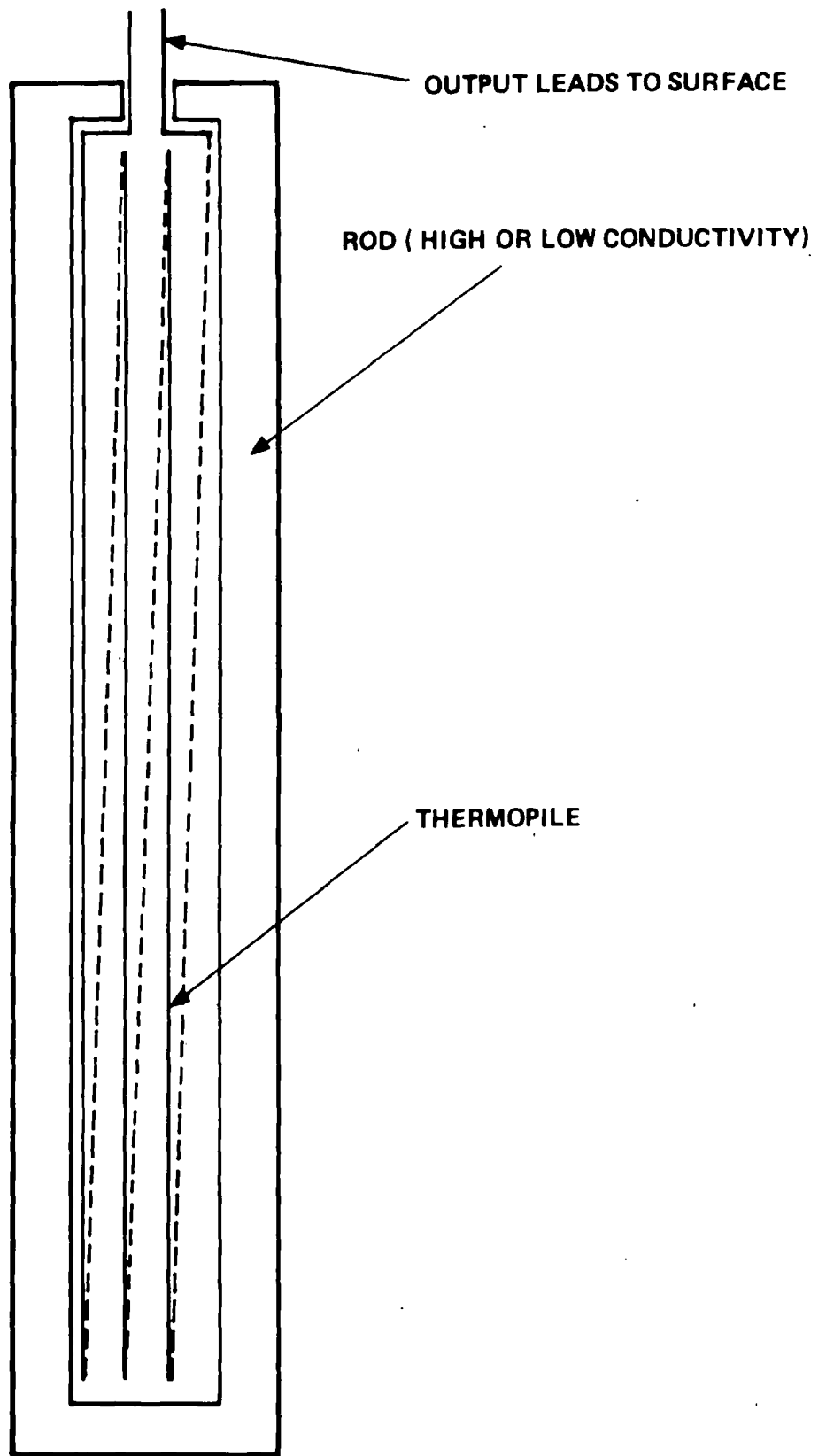
ROD (HIGH OR LOW CONDUCTIVITY)

THERMOPILE

Figure 5. Schematic drawing of the main components of the
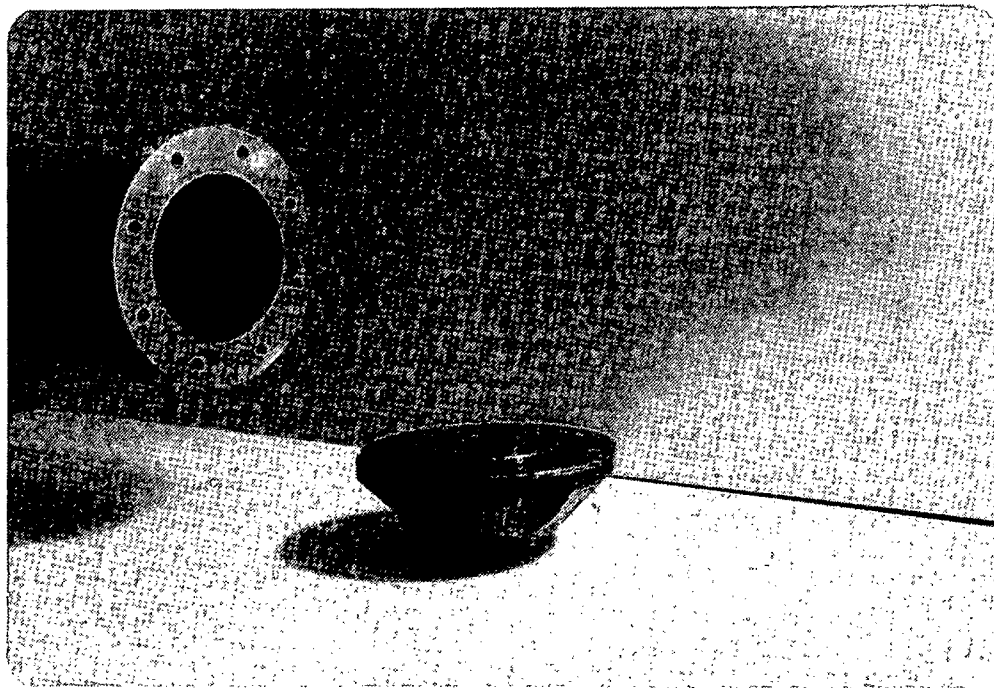rod heat flux transducer.

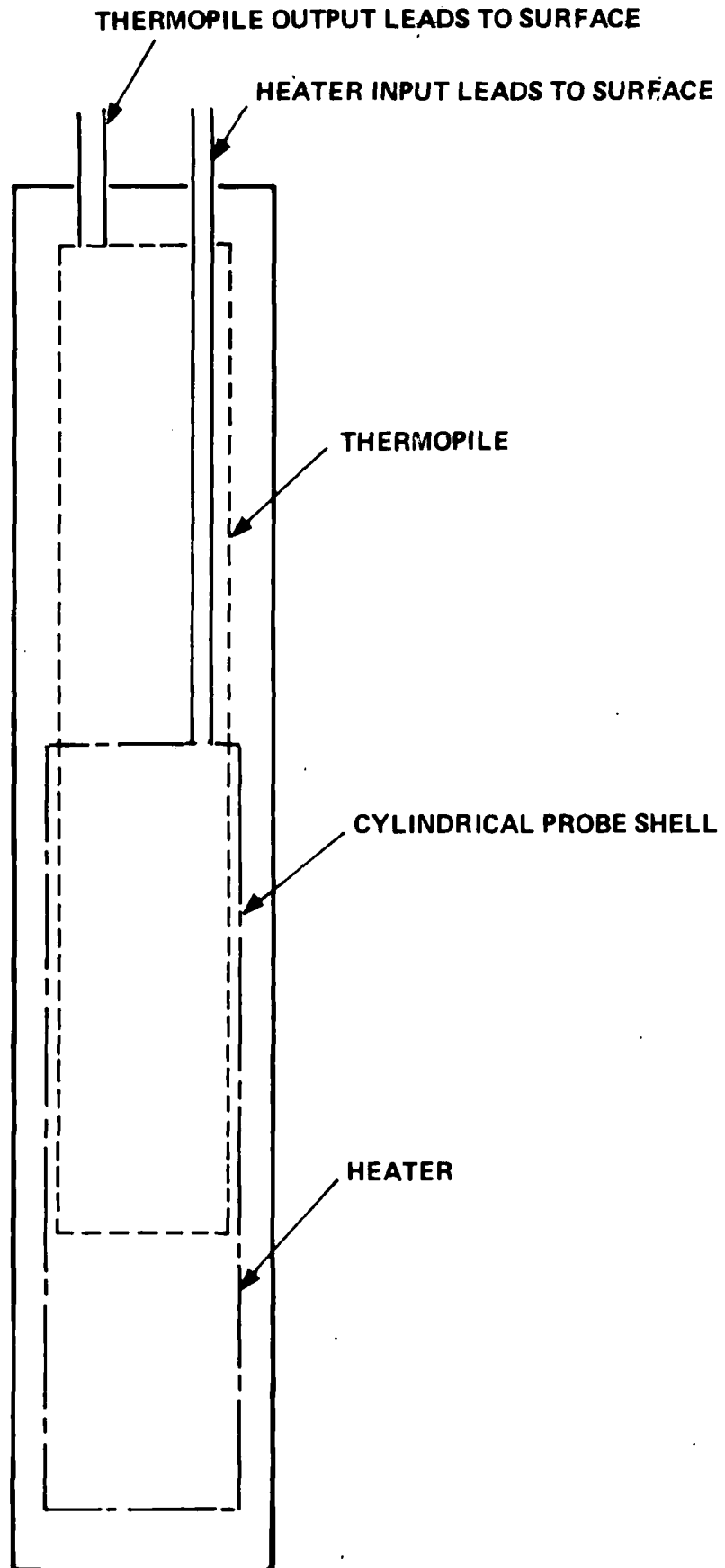Figure 6. End view of the rod heat flux transducer.

Figure 7. Schematic drawing of the main components of the thermal conductivity probe.

pressed into the large open volume. Figure 8 shows a photograph of the open shell with the installed matrix and the two sets of leads. In order to keep the current and voltage requirements of the heater within a reasonable range, the heater was divided into two parts. This was accomplished by using a center tap on the assembled strip heater so that the two halves were identical. The total heater resistance with this arrangement is 100 ohms. The heater is typically operated at 0.64 amps and 64 volts. Because of lead resistance in the seven-conductor cable to which the probe is attached, the voltage applied at the winch truck is typically 155 volts in order to maintain the current at 0.64 amps. A view of the shell with the welded end plate is shown in Figure 9; note the seven-conductor male plug which connects to the power/thermopile cable. The working drawings for this transducer have been presented previously.[7]
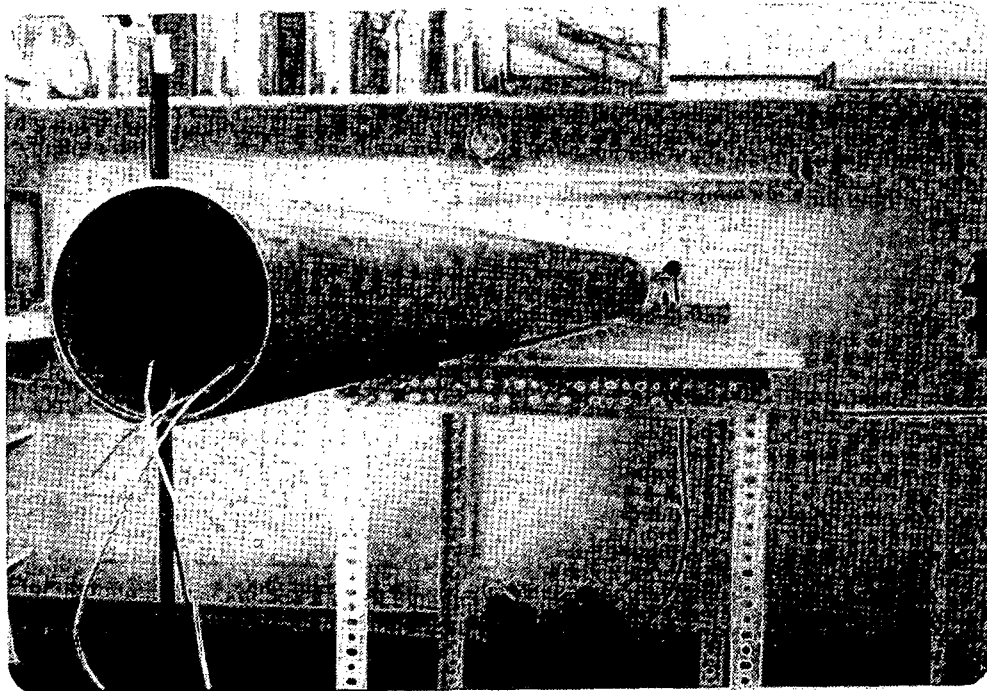
Figure 8. View of the open end of the thermal
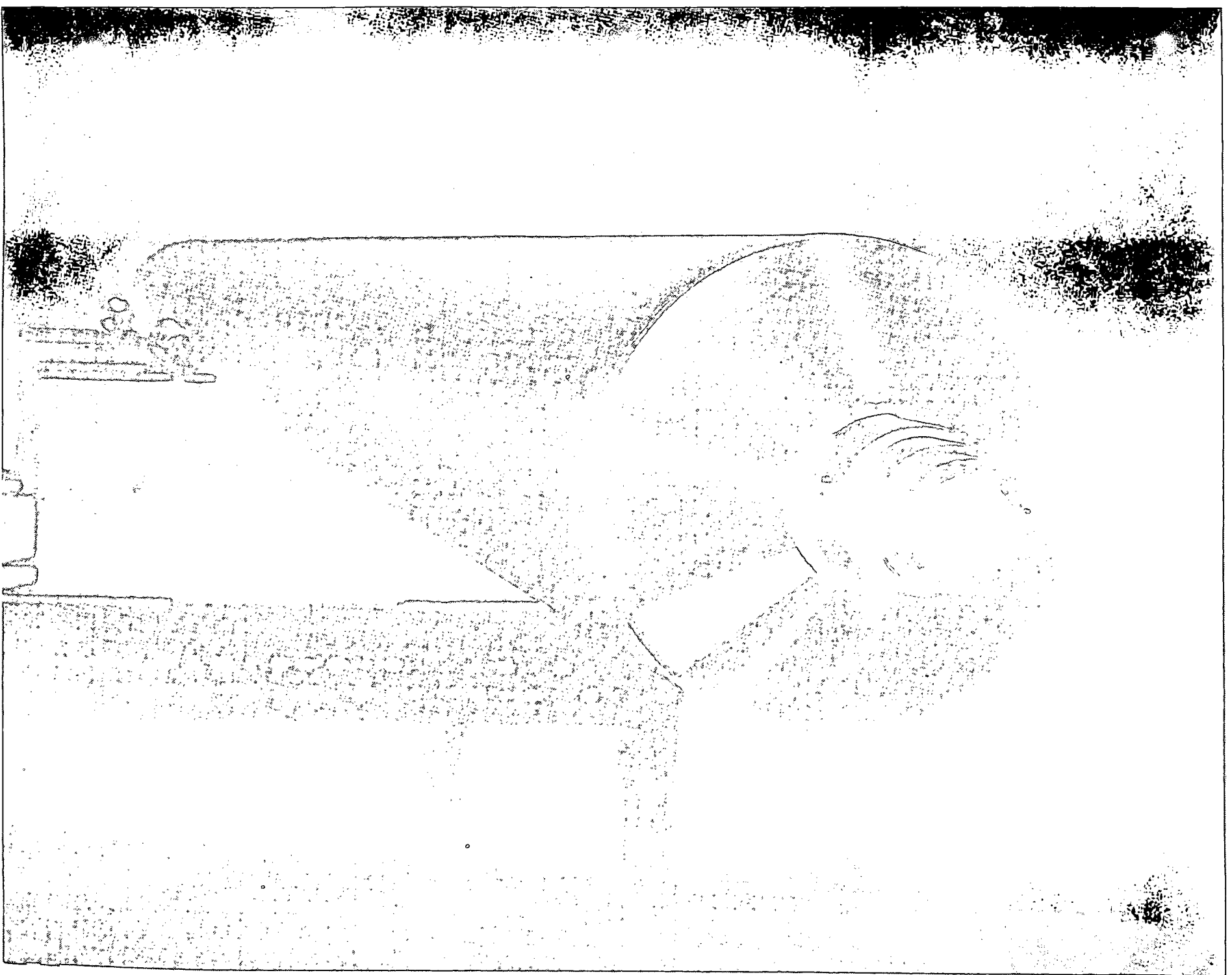conductivity probe.

Figure 9. A view of connector end of the thermal conductivity probe.

IV. GEOSCIENCE'S EQUIPMENT FOR THE DOWNHOLE TESTS

Figure 10 shows Geoscience's two downhole transducers and some of the associated support equipment that was taken to the test site. The support equipment includes potentiometric measuring instruments and instruments for monitoring the heater power. In addition, geothermal heat flux transducers that have in the past been used in mine tunnels and micrometeorological equipment were also taken. Other items shown in the figure are covers to protect the open well hole and weights used to sink the thermal conductivity probe.

Figure 11 shows the portable motor-generator set (a stand-by unit) to provide power to the heater and recorder. It is capable of handling a 3000-watt load.

Prior to the start of the downhole tests at the Phillips well, the Sandia mast truck had been driven to the site without difficulty; the heavy logging trailer, however, could not be moved to the well because of the wet conditions of the roads. Thus, the test start was significantly delayed. During the last week in April, Sandia informed Geoscience that it could no longer leave the mast truck at the well site because it had been scheduled to be used in a U.S. Geological Survey program. It was suggested that Geoscience design and fabricate a mast to perform the transducer lowering operations using two Sandia sheave wheels. Geoscience designed a tripod mast, procured the components and fabricated the system in three days prior to departure to the test site. The mast weighed 500 pounds and was capable of lifting 5,000 pounds (see Figure 12).
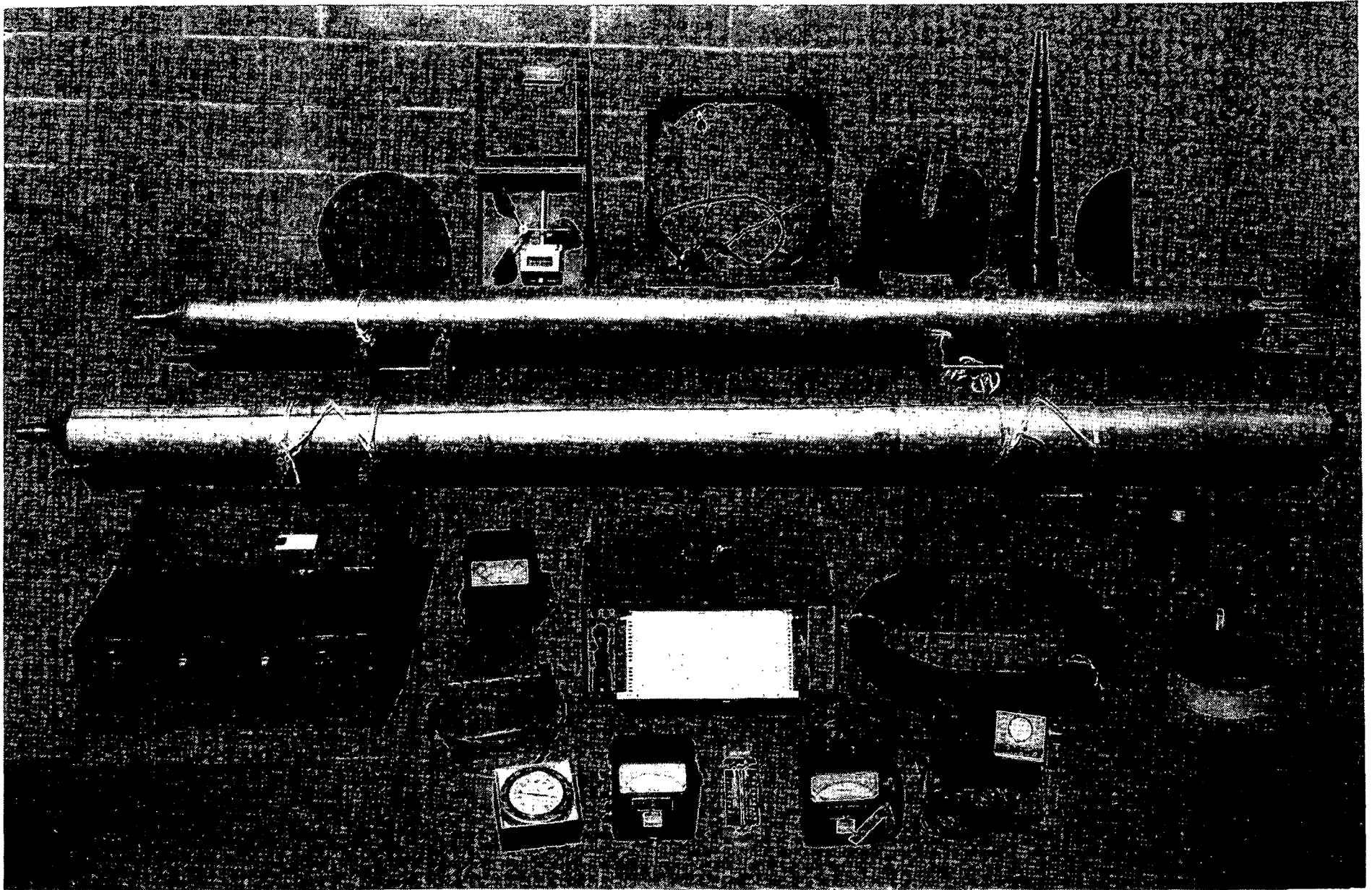
Figure 10. View of the two downhole transducers along with associated support equipment.
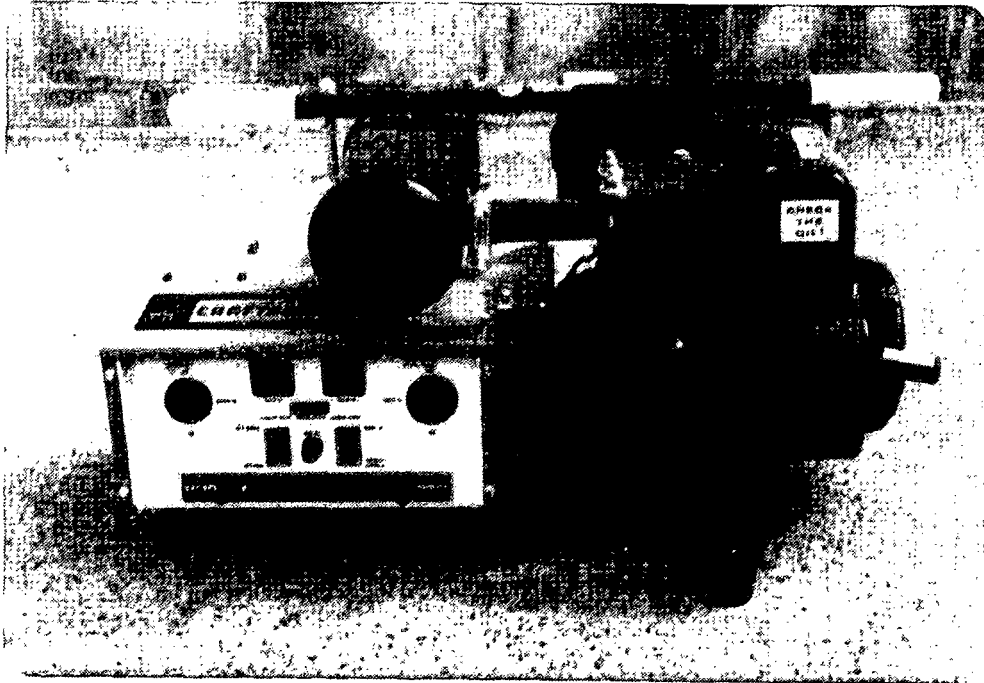
Figure 11. The standby motor generator set.

Figure 12. A photograph of the tripod mast

V. TEST SITE DESCRIPTION

The well which was used by Geoscience for these tests was located in the mountains to the west of Middletown, Sonoma County, California. It had originally been drilled by the Phillips Petroleum Company as a temperature observation well with a total depth of two thousand feet in June of 1977. The drilling log shows that clay and volcanics were the types of earth encountered to a depth of about 400 feet. Deeper than 400 feet, the rock consisted of clay and greenstone to about 1000 feet and then principally gabbro to the bottom of the hole which was almost completely filled with water; the liquid level was at about 100 feet below the surface. The well contained a steel liner surrounded by a thin cement annulus to a depth of about 300 feet; the hole was uncased from 300 feet to the bottom.

At the time of the first well probing in May 1978, it was discovered that the well had a plugged region starting at about 430 feet. Therefore, the tests of the Geoscience transducers had to be conducted within the clay and volcanic section of the well.

A photograph of the well head can be seen in Figure 13. The liner inside diameter was 6.5 inches and the original diameter of the open hole, below the liner, was 6.25 inches.
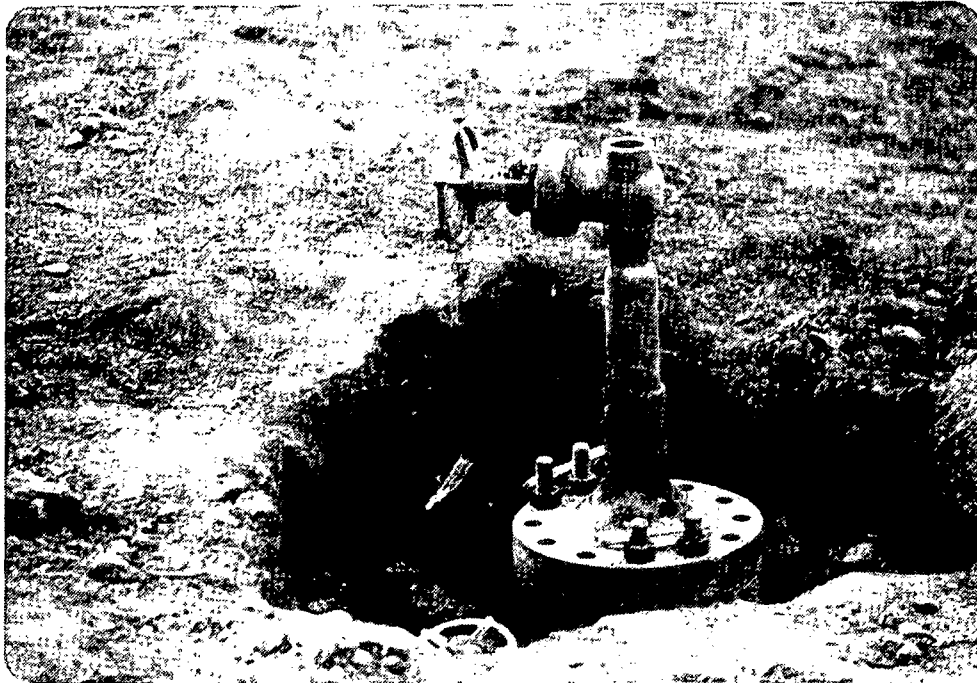
Figure 13. View of the well head

VI. TEST PROCEDURE

The following test procedure was defined for the downhole work at the Phillips well.

1. Caliper Measurements

    Verify the diameters of the liner and open hole regions of the well using the Gearhart-Owen logging tool (a Sandia and Gearhart-Owen effort).

2. Water Temperature Measurements

    Verify the water temperature profile in the well using a Gearhart-Owen temperature probe (a Sandia and Gearhart-Owen effort).

3. Steady State Downhole Transducer Measurements

    On the basis of the results from tests 1 and 2, establish the depths at which the Geoscience transducers would be deployed. Lower the aluminum rod transducer first. Take care to precondition this sensor (as well as the thermal conductivity probe) so that the equilibration times are as short as possible (no more than a few hours). After equilibrium is attained, record the thermopile output voltage and then remove the transducer. Next, lower the thermal conductivity probe to the same depth and allow it to come to equilibrium. After recording the thermopile output voltage, the steady state test is completed at that depth. Use the measurements so obtained to extract the earth thermal conductivity and vertical temperature gradient as well as the heat flux from the rod heat flux transducer theory.

4. Transient Downhole Transducer Measurements

Activate the thermal conductivity probe heater using the AC power supply and record the thermopile output voltage as a function of time for a period of about two hours. Determine from these measurements the thermal conductivity of the earth using the transient probe theory. Determine the vertical heat flux from the deduced thermal conductivity and the steady state vertical temperature gradient (obtained previously during the steady state measurements with this probe).

VII. FIELD OPERATIONS

By midday on May 1, 1978, Geoscience's truck loaded with the two geothermal transducers and the support equipment arrived at the Phillips well. The Sandia logging trailer had already been moved up to the test site by Mr. L. Nardi and associates (see Figure 14). Next, the well head was removed from the well top and the surrounding ground was leveled to accommodate the Geoscience tripod mast. A block and tackle system was then used to erect the tripod which was next pulled into position over the well; the three wooden pads that had been provided simplified the movement of the 500 pound tripod (see Figure 12). The tripod was also equipped with three staked guy lines to provide additional stability in the event of an unbalanced force application to the mast.

During the early part of May 2, Sandia and Gearhart-Owen staff members measured hole diameters and temperature profiles with caliper and temperature sensing equipment (see Figure 15). As soon as the caliper log was made (see Figure 16), it was learned that a plug of some sort existed at the 430-foot depth. A weighted, five-foot long cylinder (made of pipe fittings) had been brought along by Geoscience with the thought that it could be lowered first in the event that the hole clearances were smaller than anticipated. It was decided to use this component to try to break the plug after obtaining at least two sets of data for each transducer type in the unrestricted section of the well. One set of measurements was made in the liner region and another set in the open hole region where the thickness of the water annulus was no greater than one inch. Usually several

Figure 14. The Sandia logging trailer in position
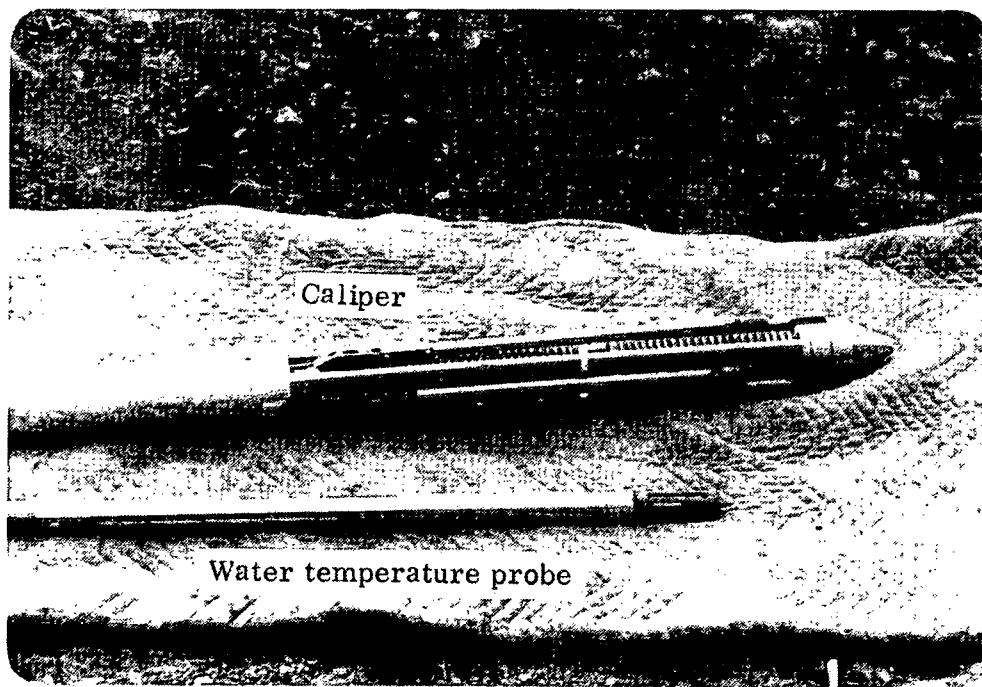at the test site.

Figure 15. A photograph of the Gearhart-Owen caliper and
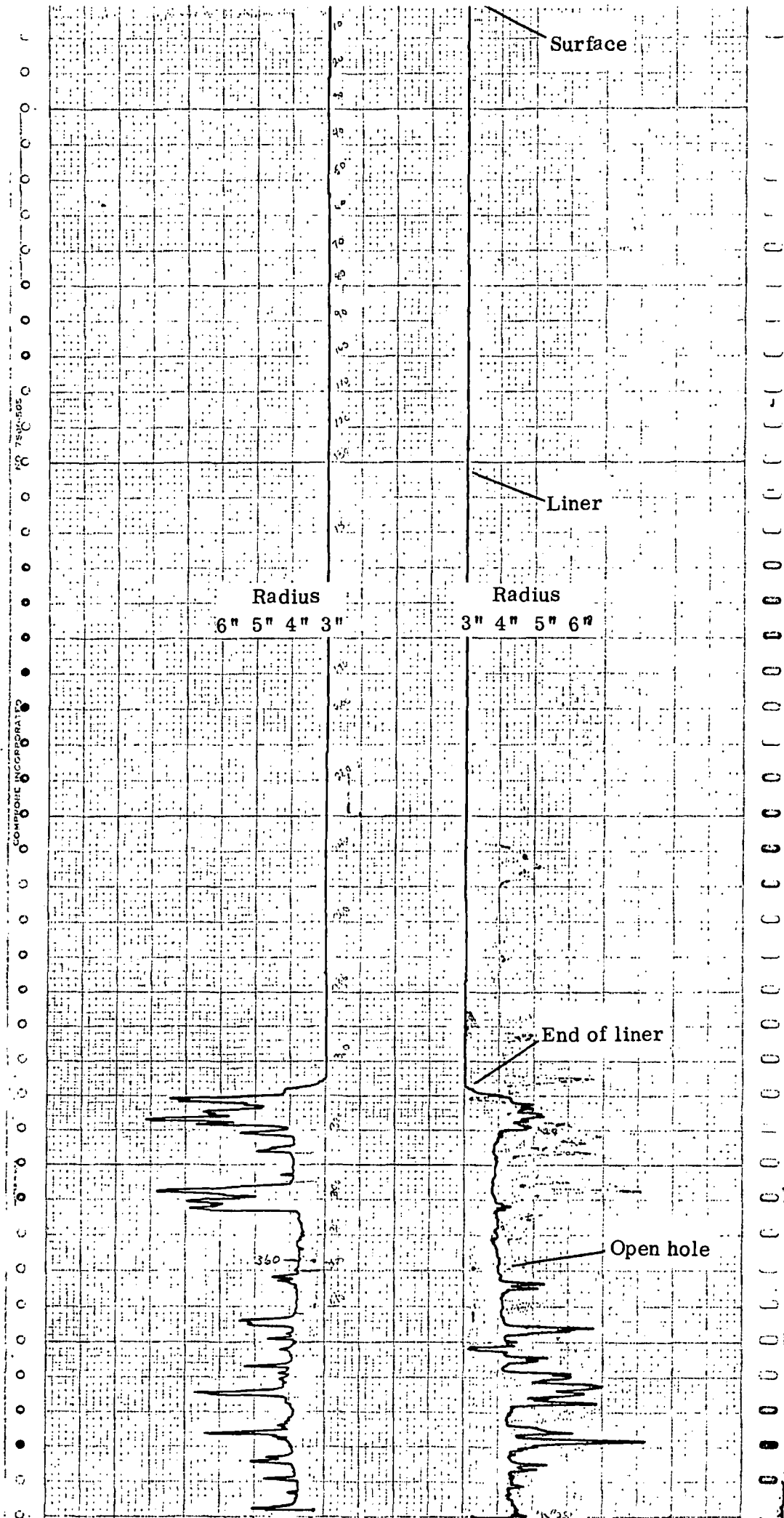water temperature probes.

Figure 16. The Sandia X-Y caliper log of the Phillips well.

hours were required for a transducer to come to equilibrium, depending upon the transducer temperature level prior to locating it at a given test depth; modest care in not allowing the transducer to overheat or overcool while on the surface prior to its use aided in preventing long equilibration times. In the case of the thermal conductivity probe, the heater was activated (for the transient run) after the steady state rod transducer run had been completed; the resulting thermopile output signal was recorded. After about an hour and a half (a time period after which two-dimensional heat flow or end fringing begins to play a role), the heater was deactivated and the decaying thermopile voltage recorded with time.

The photograph in Figure 17 depicts the rod heat flux transducer on the ground ready for exchange with the thermal conductivity probe (which is being removed from the well).

Figure 18 shows the thermal conductivity probe suspended above the well by the tripod mast after having just been raised after a transient run.

After the two data sets had been taken, the weighted, dummy cylinder was allowed to strike the plug in the well at free-fall speeds. After a number of trials with no evidence of a breakthrough, it was clear that it would not be possible to make measurements below the 430-foot depth. Thus, it was decided to make three additional measurement sets in the well above the plug (another set in the liner region and two sets in the open hole section in thick water annulus regions).
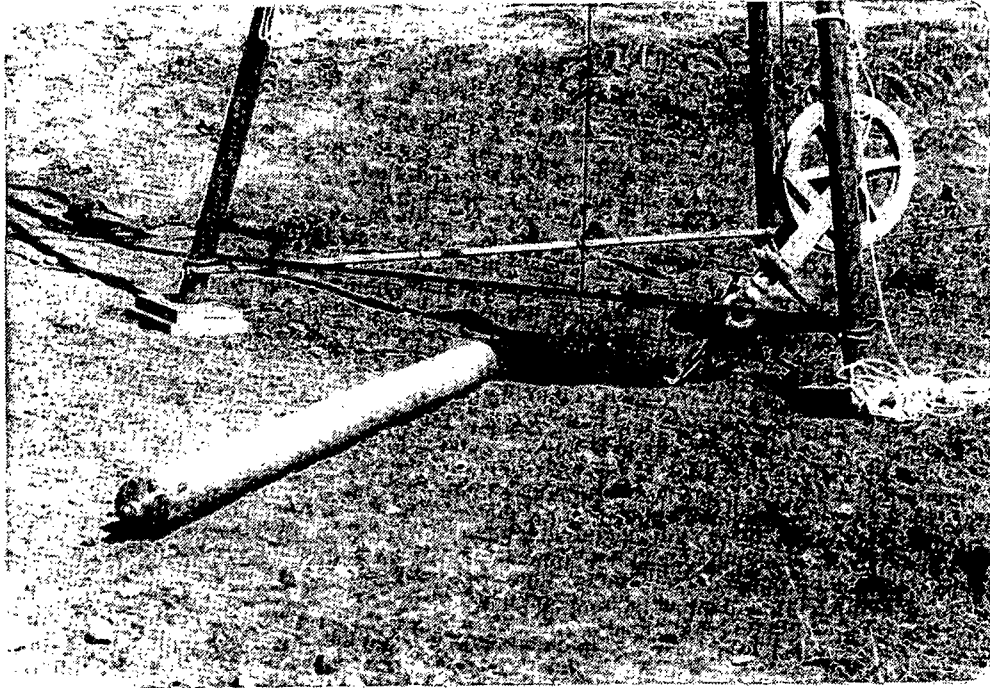
Figure 17. View of cable and rod heat flux transducer.

Figure 18. View of thermal conductivity probe just after having been removed from well.

After the completion of the Middletown measurement effort on May 6, Geoscience made sure that the roads used in getting to the Phillips well and the well site were properly cleaned up; arrangements were also made with Mr. Nardi to level the roads where damage had been done.

VIII. DOWNHOLE MEASUREMENTS

A. Well Temperature Profiles

In August of 1977, the Phillips Petroleum Company made a temperature log of the exploration hole under study. The results can be seen in Figure 19. It is of interest to compare the Phillips profile to the one obtained by Sandia on May 2, 1978, which is shown in Figure 20. The difference in the profiles, particularly at the shallower depth, are believed to be related to the differences in the annual surface temperatures as well as the heavy rainfall in April of 1978. From limited ground surface temperature measurements, a mean surface temperature value was obtained which was in agreement with a linearly extrapolated value using the profile in Figure 20.

B. Well Temperature Gradients

The vertical temperature gradients for the well were obtained from the respective temperature profiles (see Figure 21). The individual points for the Phillips profile are not shown; they exhibit more scatter than do those for the Sandia profile. For purposes of comparison, the temperature gradients as measured by the Geoscience low thermal conductivity rod heat flow transducer, are shown in Figure 22 with the Sandia curve. Although the two curves are similar, there is a significant difference in the depth at which the two curves markedly drop in magnitude. This difference (which is evaluated in a subsequent section) is related to the thermal lag in the Gearhart-Owen temperature probe. The solid points
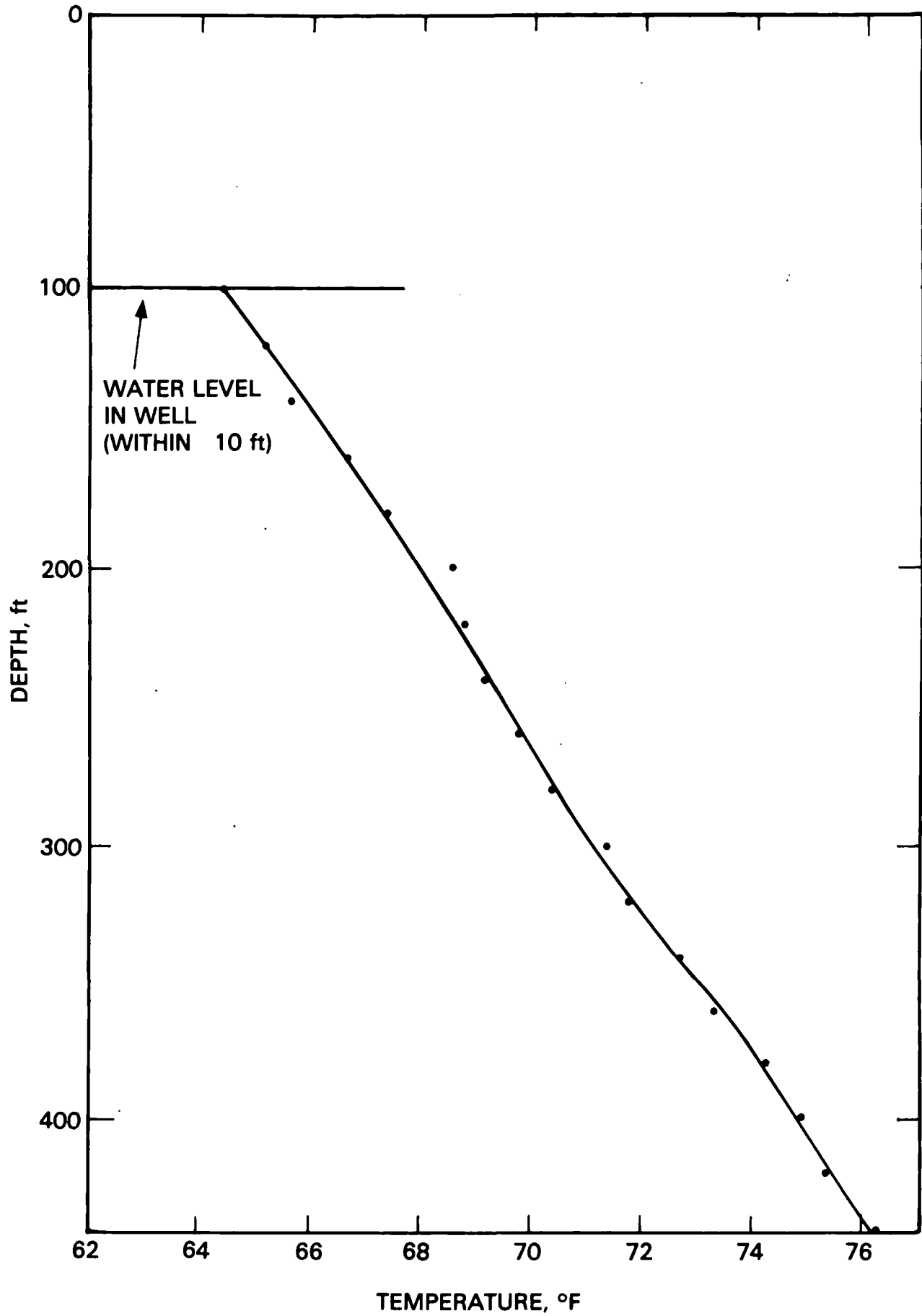
Figure 19. Well temperature profile measured by Phillips Petroleum Company on August 5, 1977.
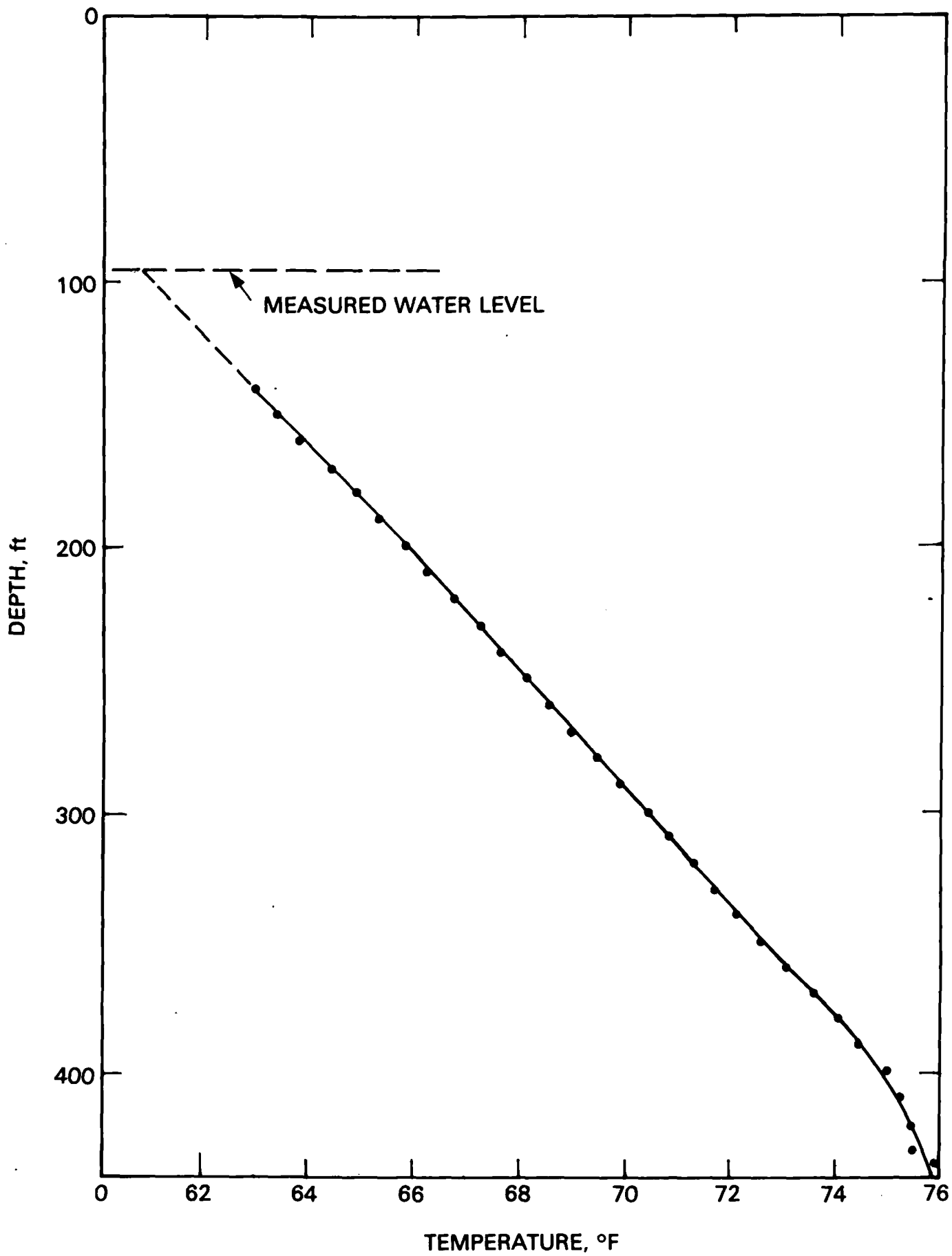
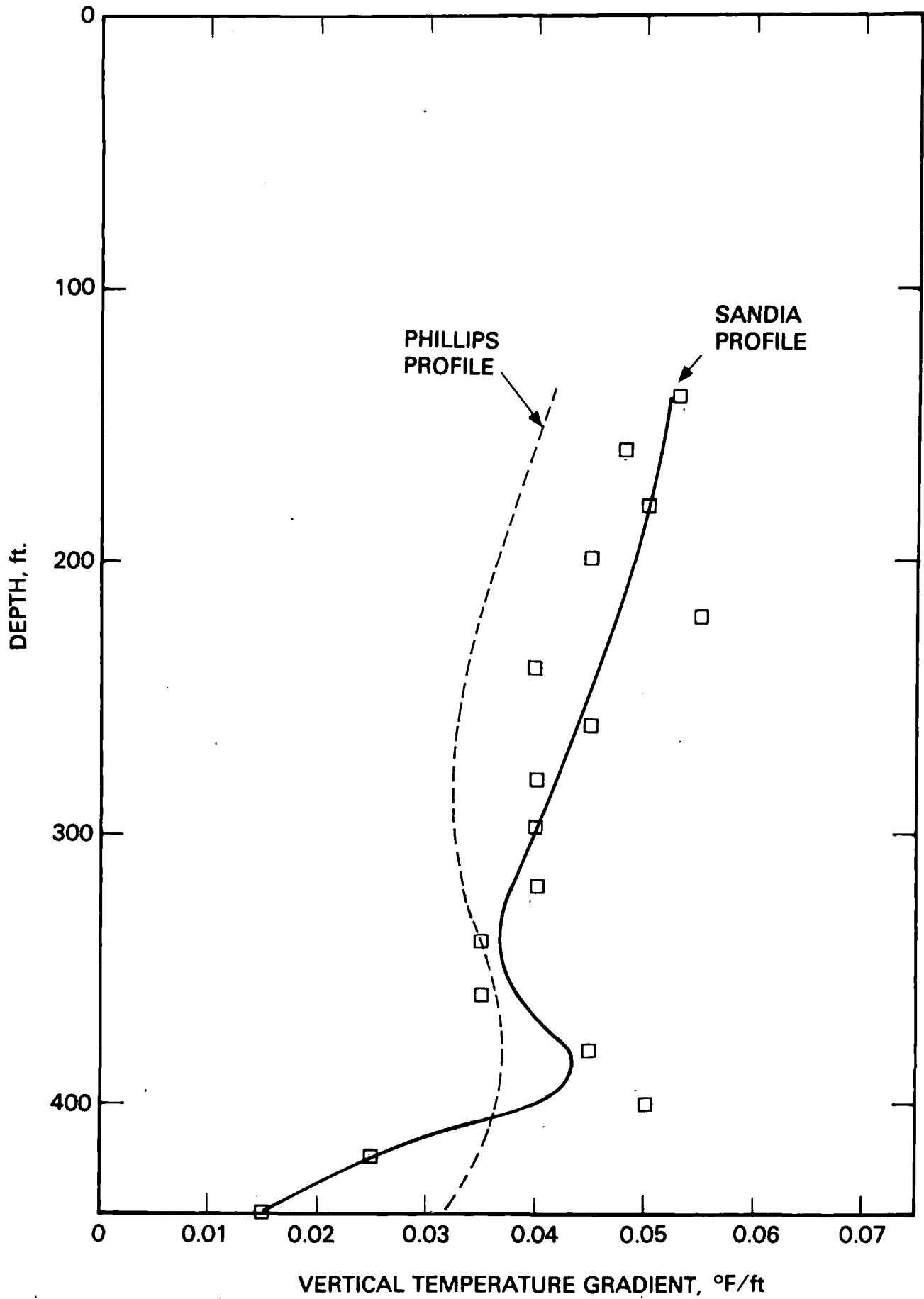Figure 20. Well temperature profile measured by Sandia on
May 2, 1978.

Figure 21. Well temperature gradients from Phillips and
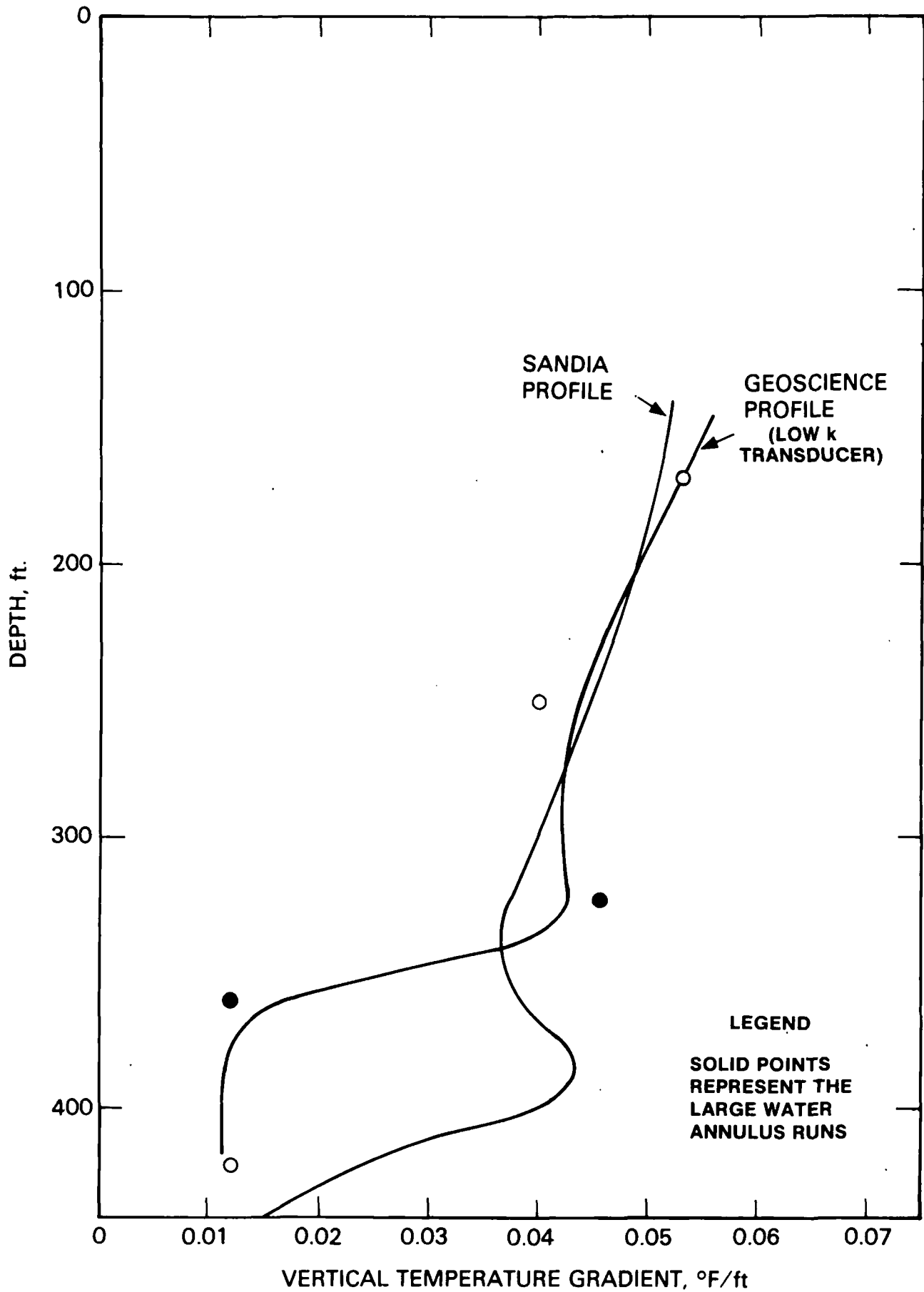Sandia temperature profiles.

Figure 22. Well temperature gradients as measured by Geoscience
and Sandia.

on the Geoscience temperature gradient curve correspond to the two large water annulus runs; these gradients can be in error by perhaps ten percent because of the water convection effects noted for these conditions.

C.   Rod Heat Flux Transducer Measurements

Figure 23 shows a circuit diagram for the rod heat flux transducer system. The thermopile leads from the transducer are connected to two of the terminals in the cablehead of the seven conductor Sandia cable. The conductors lead through a slip ring assembly in the winch to female banana plugs in the terminal panel inside the cab of the Sandia logging trailer. Several alternative methods were provided for reading the thermopile output signal. A Keithley digital multimeter was used as the primary readout instrument. This meter was frequently checked with a Hewlett-Packard digital multimeter and a manually operated Leeds & Northrup 8662 potentiometer.

The results of the rod heat flux transducer runs are shown in Table I. The two data sets marked with brackets correspond to the large water annulus cases which, as noted previously, were influenced by water convection currents that introduced errors in the measurements. This feature is discussed in a later section of this report.

D.   Thermal Conductivity Probe Measurements

The circuit for the thermal conductivity probe, a diagram of which is shown in Figure 24, is more complex than that of the rod heat flux transducer. The two thermopile leads were connected to two of the seven cable conductors. Because of the relatively high resistance of the cable
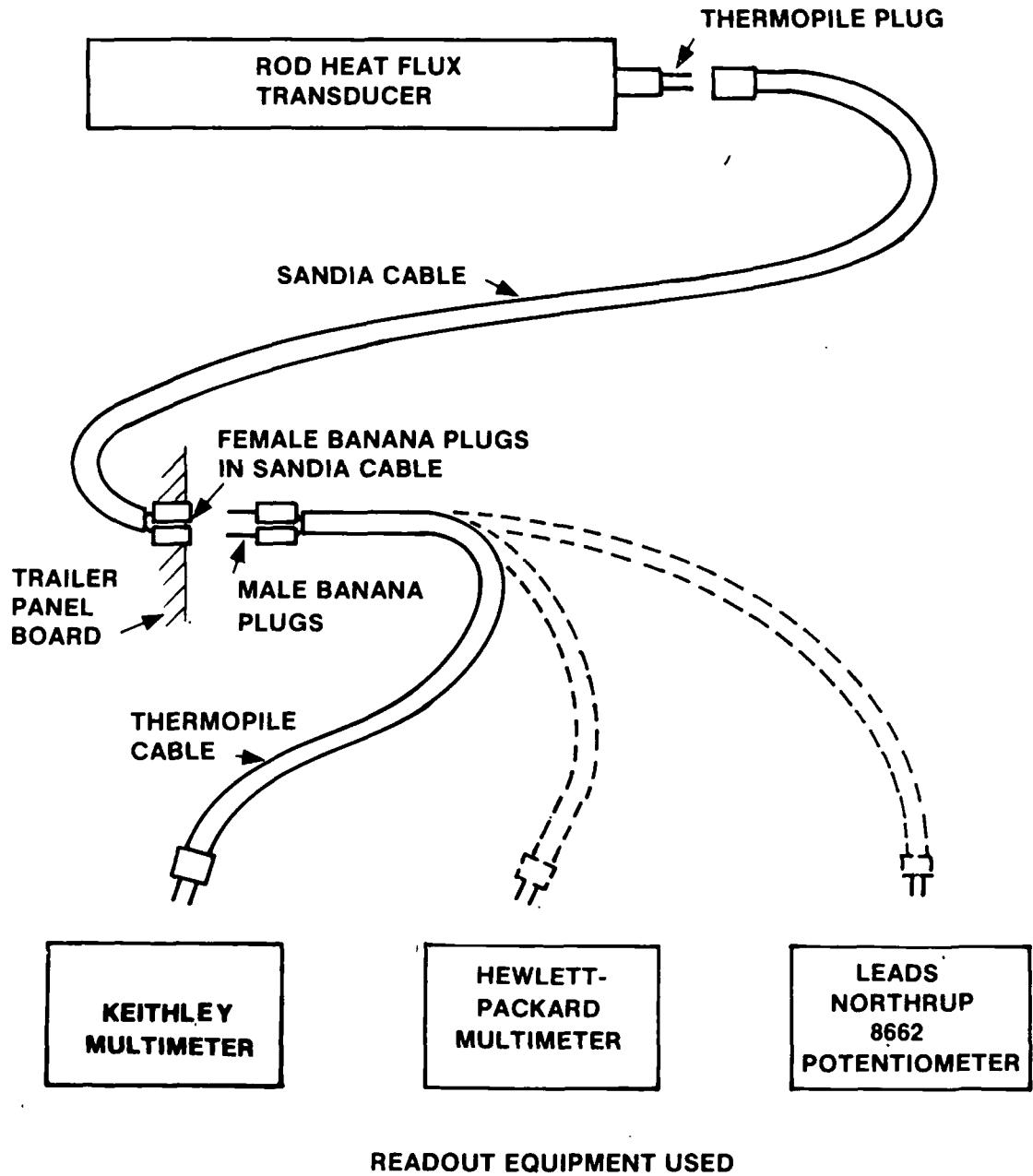
Figure 23. Circuit diagram for the rod heat flux transducer.

TABLE I.

Thermopile Output Voltages for the
Low and High Conductivity
Rod Heat Flux Transducers

Depth ft	Annulus Thickness inches	E_{low} mv	E_{high} mv
170	0.5	0.28	0.32
250	0.5	0.21	0.44
326	~1.8	[0.24]	[0.47]
362	~1.0	0.065	0.105
423	~1.4	[0.065]	[0.15]

Figure 24. Circuit diagram for the thermal conductivity probe.

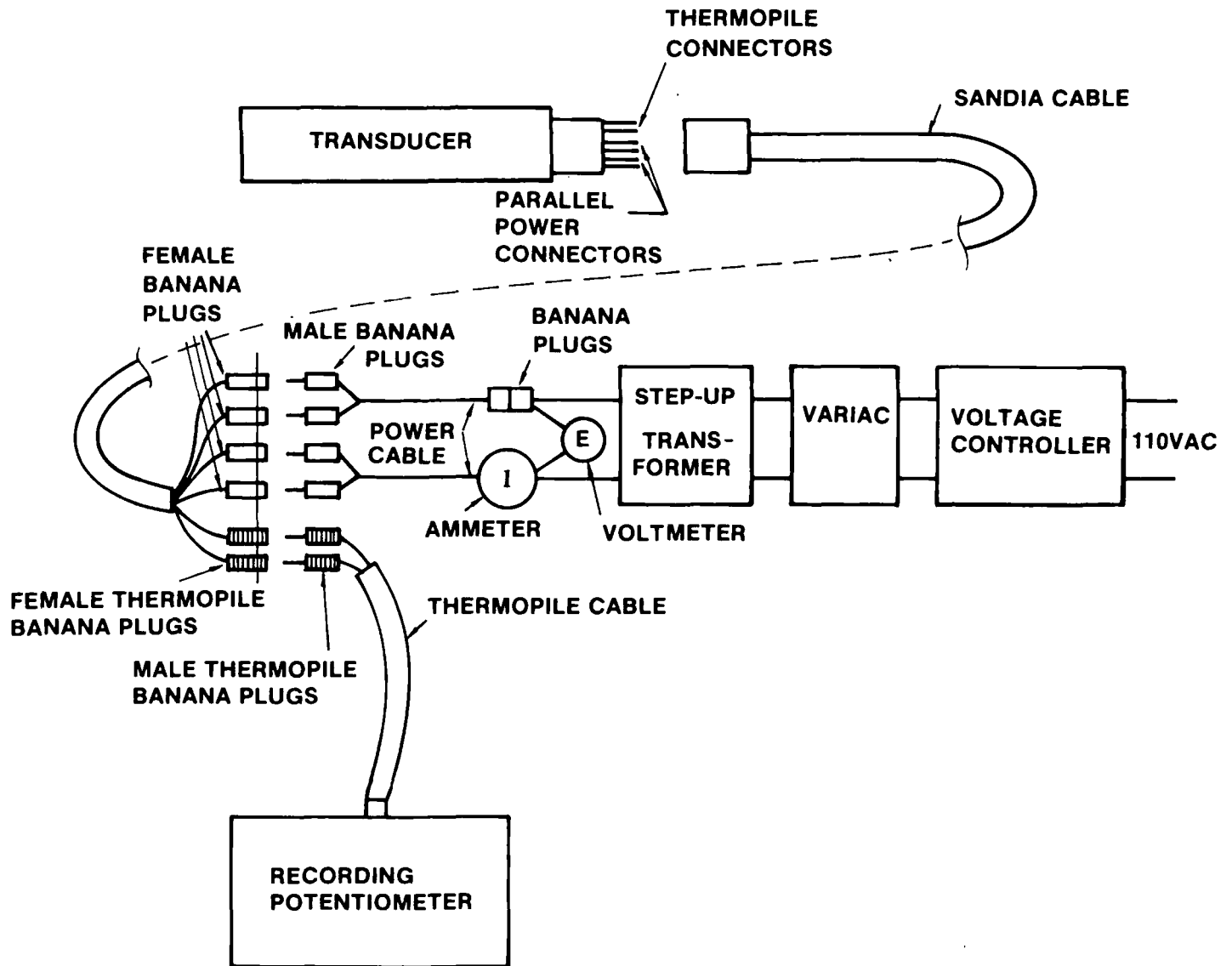conductors, the two power leads from the probe were each connected to two cable conductors operating in parallel. Therefore, four of the cable conductors were used for power transmission. The conductors were led into the Sandia logging trailer cab where they terminated in a banana plug panel. From this panel the thermopile leads were connected through a short cable to a Honeywell chart recorder which made a record of the thermopile output voltage versus time. This recorder was checked occasionally for accuracy using the other potentiometric instruments which were available. The power lines were connected with another short cable to the power supply. The Sandia logging trailer was equipped with a 110 volt AC motor-generator set which was the basic power source for all the electrical equipment. Power for the thermal conductivity probe heater was taken from the motor-generator set and ducted through a controlling variable autotransformer which, in turn, powered a step-up transformer to give a 220 volt AC capability. A voltage controller was available in case of voltage fluctuations but the output of the motor-generator set proved to be so steady that the voltage controller was not used. The power leads from the step-up transformer were connected directly to the Sandia cable and thence to the transducer heater. The power was monitored continuously using a calibrated laboratory voltmeter and ammeter.

The recording potentiometer and a digital multimeter can be seen in the photograph of Figure 25. An alternate digital multimeter which was used primarily to read the rod heat flux transducer thermopile output voltage is shown in Figure 26.
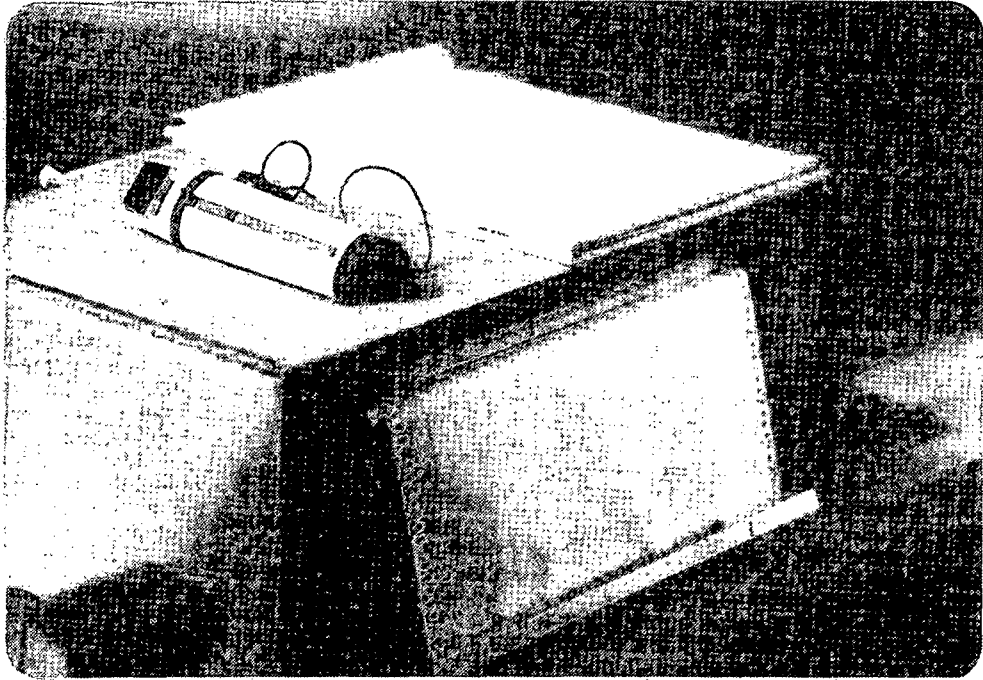
Figure 25. Honeywell recording potentiometer and a Hewlett-Packard multimeter.
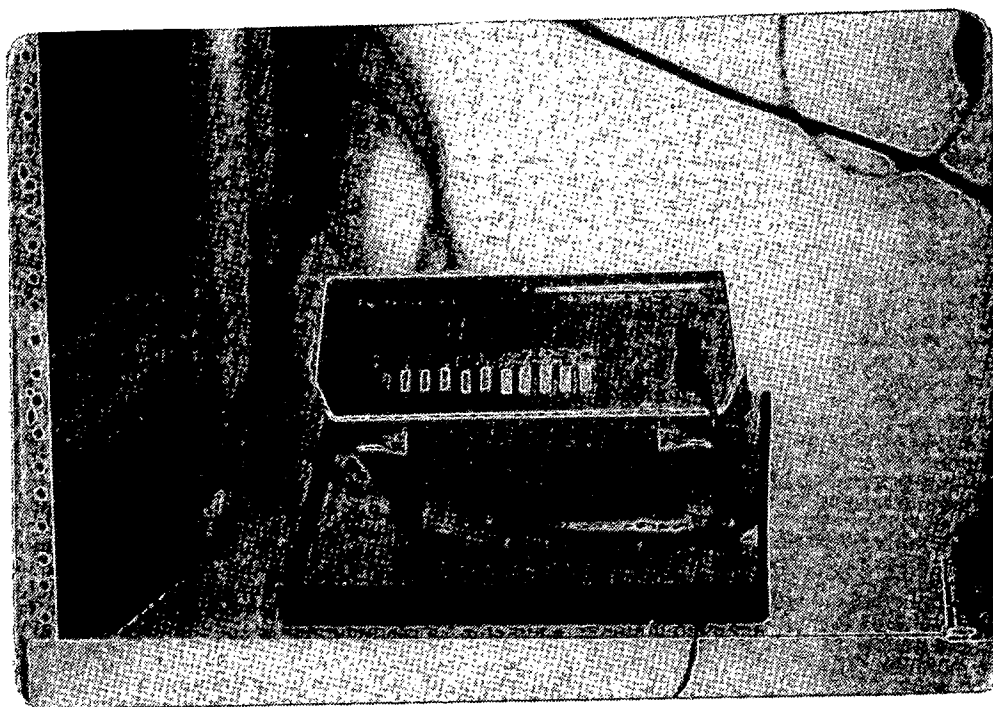
Figure 26. Keithley multimeter.

The thermal conductivity probe transient heating runs produced time versus temperature rise curves such as those illustrated in Figures 27 and 28. Note that Figure 28 shows some deviation from a smooth curve during the later stages of heating. This type of deviation is typical of the data taken where large water annuli existed and is thought to be due to convection currents in the water surrounding the transducer.

Figure 27. Probe temperature rise versus time at a 170-foot
depth (water annulus thickness about 0.5 inches).

Figure 28. Probe temperature rise versus time at the 423-foot depth (water annulus thickness about 1.4 inches).

IX. RESULTS

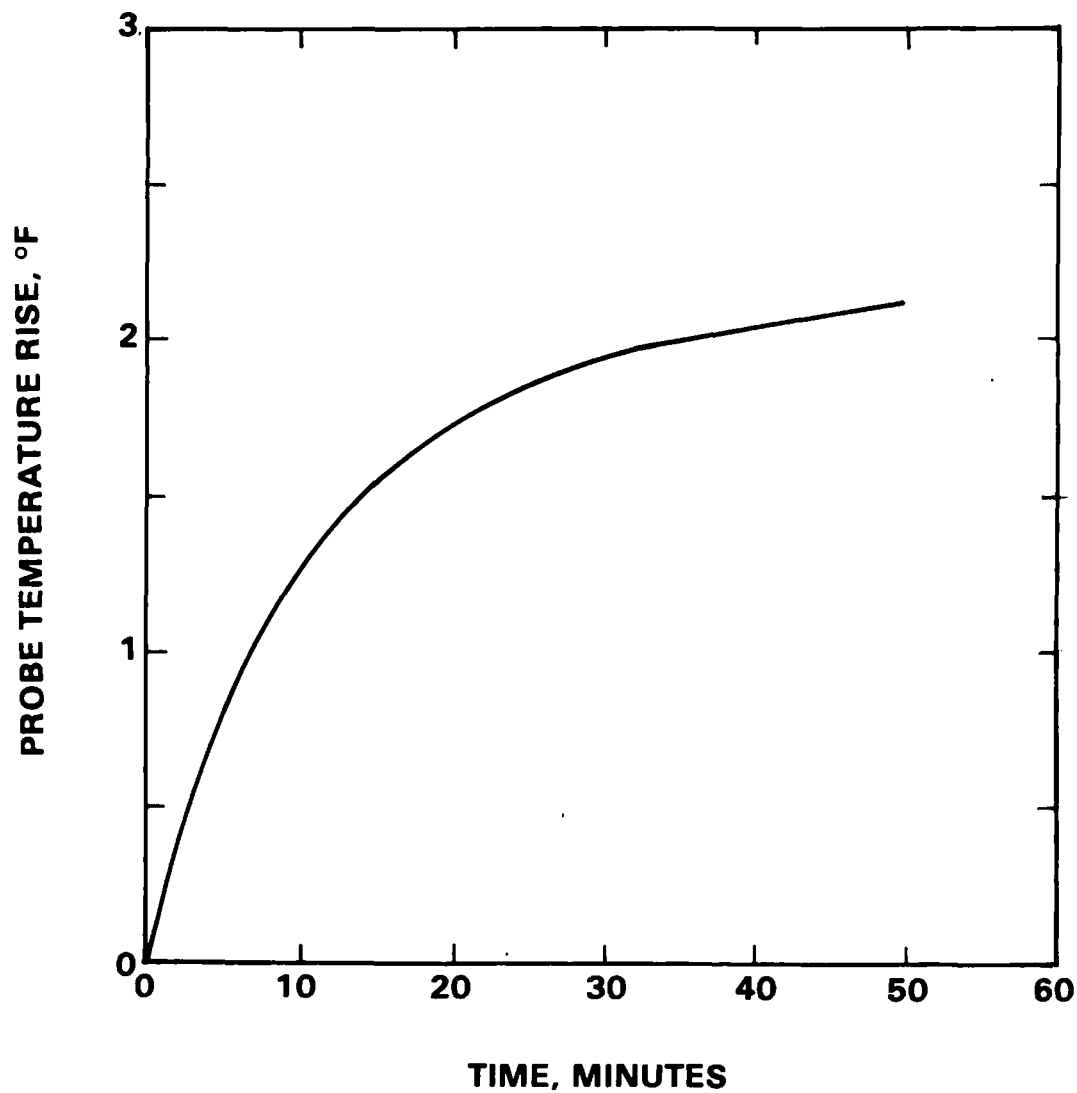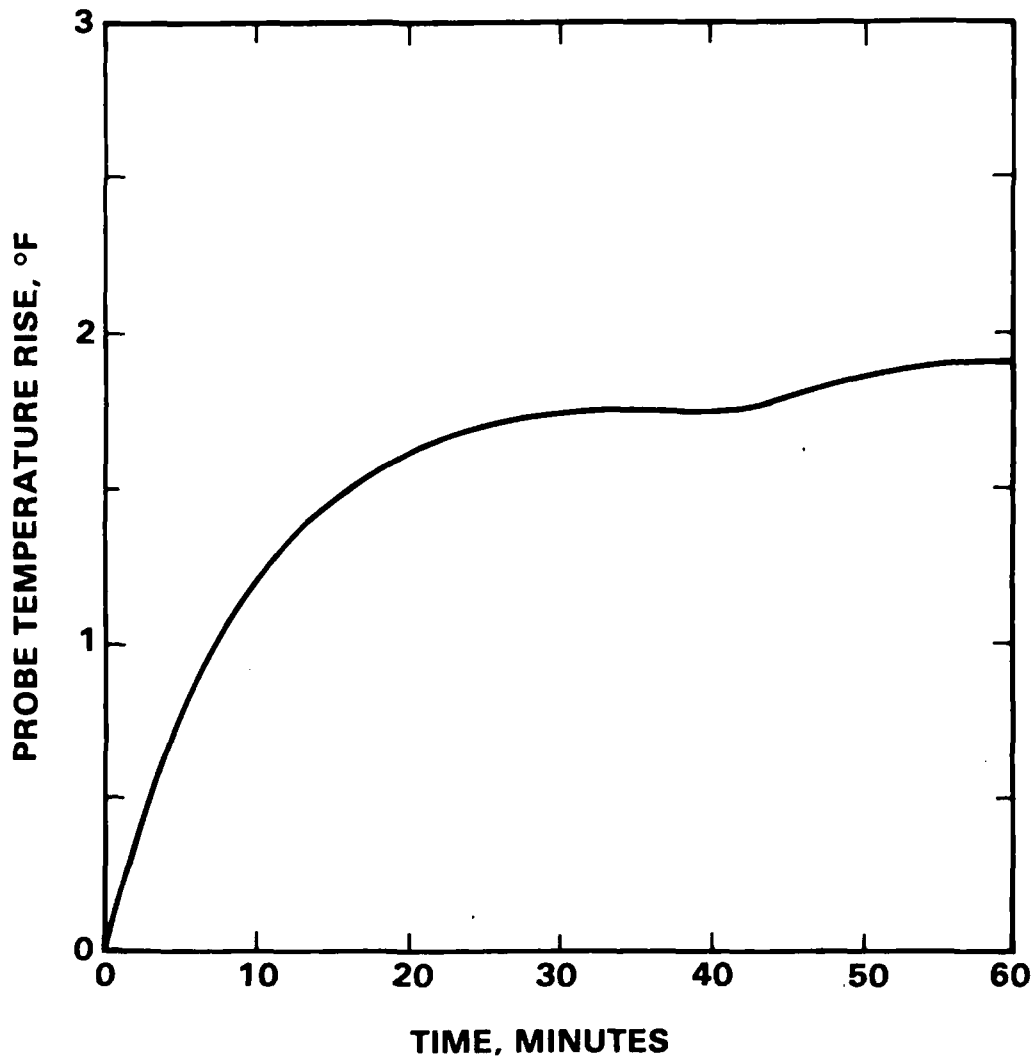A. Rod Heat Flux Transducer

Calculations were made for the rod heat flux transducer data using the equations given in the Appendix of this report. The thermal conductivities and geothermal heat fluxes at various depths that resulted from these calculations are given in Table II. Results are presented only for the three cases in which the annuli were relatively thin (about one inch or less).

B. Thermal Conductivity Probe

Calculations were made using the data derived from the thermal conductivity probe using the methods given in the Appendix of this report. The data produced by the thermal conductivity probe have been corrected for the temperature difference across the shell of the probe. Because of the construction of the probe, consisting of (1) a layer of Teflon insulation between the thermopile and the outer shell, (2) a small air gap, and (3) the outer shell itself, the thermopile does not measure the outer surface temperature. Accounting for the Teflon insulation and a small representative air gap between the thermopile and the outer shell and assuming that the temperature drop across the shell itself is negligible, a temperature drop from the thermopile to the surface of the transducer was calculated and found to be about one degree Fahrenheit for the heater powers used at the test site. The temperature drop between the thermopile and the outer surface was also measured in the laboratory. This

TABLE II.

Rod Heat Flux Transducer Results

$$r_o = 3 \text{ ft}$$

Depth ft	k_∞		q/A (HFU)
	(Btu/hr ft^2 (°F/ft))	(cal/sec cm^2 (°C/cm))	μ-cal/sec cm^2
170	0.65	2.7×10^{-3}	2.6
250	0.70	2.9×10^{-3}	2.3
362	2.67	11.0×10^{-3}	2.4

difference was found to be 0.75°F and this value was used to evaluate

the probe surface temperature variation. The results of these calcu-

lations are shown in Table III. Again, calculations were made only

for the thin annulus cases. The thermal capacity per unit volume

$(\rho_\infty c_{p_\infty})$ is also shown in Table III, as it is also a parameter in the

evaluation analysis as is the thermal conductivity.

C.   Supplementary Measurements

While the downhole transducer tests were in progress at the Phillips

well, Geoscience made an attempt to find a mine tunnel somewhere in

the vicinity of the test site so that one of Geoscience's flat heat flux

transducers could be used to make a direct measurement of the heat

flux in such a tunnel. Two mine tunnels were identified. The Helen mine,

which was located at some distance from the well site, was sealed and

thus could not be used. The second mine tunnel which was a short

distance from the test site was dangerous and Geoscience was advised

by the owners not to enter the tunnel. During the last days of the test

effort, a shallow tunnel (about 20 feet below the surface) was located

nearby. Geoscience was allowed to make temperature and heat flux

measurements in this tunnel; however, this site was not adequate. The

tunnel was only about 50 feet long and, therefore, its temperatures were

influenced by diurnal outside air temperature variations. Thus, only

an approximate, mean heat flux could be determined in this tunnel.

The mean temperature measured in the tunnel fell near the extrapolated

surface temperature obtained from the Sandia temperature profile. An

TABLE III.

Thermal Conductivity Probe Results

Depth ft	$\rho_\infty c_{p_\infty}$ Btu/ft^3 °F	k_∞		q/A (HFU)
		(Btu/hr ft^2 (°F/ft)	(cal/sec cm^2 (°C/cm)	μ- cal/sec cm^2
170	30	0.7	2.9×10^{-3}	2.6
250	35	0.7	2.9×10^{-3}	2.3
362	17	2.1	8.7×10^{-3}	1.9

approximate mean heat flux measurement for the tunnel was two to three times higher than the downhole heat flux measurements. This result was to be expected because of the seasonal heat flow function at that shallow depth as well as the previously noted evaporative effect.

X. DISCUSSION OF THE RESULTS

It is of interest to compare the well temperature profiles as measured by
the Phillips Company and Sandia (see Figures 19 and 20). It is noted that
the water level in the well had not changed in the interval between measure-
ments. The temperatures in the upper layers of the earth were, however,
lower in the Sandia profile than those obtained by Phillips. It is believed
that this difference exists because of the additional evaporative cooling from
the surface as a result of the heavy rains that had occurred prior to tests
and because of seasonal effects. At the lower depths, the Phillips and
Sandia well temperature profiles were in agreement.

It is also of interest to compare the well temperature gradients shown in
Figure 22 as determined by Sandia and by Geoscience (via the low thermal
conductivity rod heat flux transducer). Although the two curves are similar,
it is clear that the depth at which a rapid decrease in the temperature gradient
occurs differs for the two profiles. As indicated previously, it is believed
that this difference is related to the time lag that exists for the Gearhart-
Owen temperature logging probe as it is being lowered in the well at a rate
of 30 feet per minute. A transient conduction analysis was made for an
idealized tube of water (a boundary layer region) around the probe
when exposed to a temperature step function change of the environmental
well water. The results indicated that the $1/e$ time constant for this system
is about 1.8 minutes if it is presumed that the eddy thermal conductivity of
the water in the tube is ten times the molecular value. This approximate

time constant calculation is in reasonable agreement with the actual two-minute lag noted in Figure 22 between the Sandia and Geoscience measurements in the region of sudden decrease in the temperature gradient.

As indicated previously, it is believed that water convection patterns generated thermal noise in the two test runs where large water annuli existed. Specifically, it was noted for both the high and low conductivity rod heat flux transducers that time variations in the output signal existed. Therefore, the thermopile voltage (or temperature difference) ratios, for the large annulus cases, were not accurately determined. Hence, the thermal conductivity and heat flux calculations were not made for these two cases.

The thermal conductivity range for the type of rock described by Phillips for its well ranged from approximately $0.3 < k_{\infty} < 2.0$ Btu/hr ft^2 (°F/ft).[8] The measured test site k values presented in this document fall within the range of $0.65 < k_{\infty} < 2.7$ Btu/hr ft^2 (°F/ft).

The lower $\rho_{\infty} c_{p_{\infty}}$ value at the 362-foot depth that resulted from the thermal conductivity probe calculations (see Table III) is believed to be related to a change in rock structure at that level. The Geoscience results were reviewed by the Phillips Petroleum Company and Phillips staff members reported to Geoscience that a change in lithology occurred near the 400-foot depth. For example, if clays are abundant, as indicated in the drilling log, it is expected that the density would then be lowered to the range 112 to 150 lb/ft^3; the specific heat, however, would not change significantly, remaining approximately 0.22 Btu/lb °F. Further, the thermal conductivity of clays is

about 2 Btu/hr ft^2 °F; this value agrees with the thermal conductivity measured at the 362-foot depth by the two methods used.

The comparison of thermal conductivity and heat flux results as measured by the two different transducers (Table II and Table III) appears to be satisfactory. Therefore, Geoscience feels that both instruments tested can play a role in downhole thermal conductivity and heat flux measurement efforts in future geothermal exploration evaluations.

XI. ACKNOWLEDGMENTS

Larry and Jim.

XII. REFERENCES

1. Goss, R., and J. Combs, "Thermal Conductivity Measurement and Prediction from Geophysical Well Log Parameters with Borehole Application, " in Proceedings, Second United Nations Symposium on the Development and Use of Geothermal Resources, Vol 2, p 1019, U. S. Government Printing Office, 1975.

2. Kappelmeyer, O., and R. Haenel, Geothermics, with Special Reference to Application, Gebrüder Borntraeger, 1974.

3. Poppendiek, H. F., and D. J. Connelly, "A Thin Rod Heat Flux Transducer Positioned in the Earth Having A Uniform Temperature Gradient: A Closed Form Solution, " GLR-178, February 1977.

4. Poppendiek, H. F., and D. J. Connelly, "Cylindrical and Spherical Transient Heat Transfer Solutions and Their Application to Thermal Conductivity Measurements in the Earth, " GLR-185, February 1977.

5. Poppendiek, H. F., and D. J. Connelly, "The Effects of a Fluid Annulus on the Performance of Thermal Transducers in a Borehole: Sensitivity Analyses, " GLR-189, August 1977.

6. Proceedings, Second United Nations Symposium on the Development and Use of Geothermal Resources, U. S. Government Printing Office, 1975.

7. Sellers, A. J., D. J. Connelly, H. F. Poppendiek, and C. M. Sabin, "Summary of Geoscience's Design Studies for the Rod Heat Flux Transducer and the Thermal Conductivity Probe, " GLR-192, Aug 1977.

8. Jumikis, A. F., Thermal Soil Mechanics, Rutgers University Press, 1966.

XIII. NOMENCLATURE

A , cross sectional area of the rod

a , thickness of the thin slab

b , undisturbed vertical temperature gradient in the earth

c_{p_∞} , specific heat of the earth

D_1 , thermal diffusivity of the thin slab

D_2 , thermal diffusivity of the semi-infinite solid

k , thermal conductivity of the rod

k_1 , thermal conductivity of the thin slab

k_2 , thermal conductivity of the semi-infinite solid

k_∞ , $\begin{cases} \text{thermal conductivity of the infinite solid} \\ \text{thermal conductivity of the earth} \end{cases}$

ℓ , half length of the rod

P , perimeter of the rod

q , the constant heat release per unit length

$\left(\dfrac{q}{A}\right)_0$, constant heat flux addition at $x = 0$

r , radial distance from the cylinder centerline

r_i , radius of the rod

r_o , $\begin{cases} \text{radius at which the undisturbed linear temperature field in the infinite} \\ \text{solid exists} \\[6pt] \text{radius of the cylinder} \end{cases}$

R_e , equivalent end thermal resistance of the solid surrounding the rod

R_∞ , equivalent radial thermal resistance of the solid surrounding the rod

t , $\begin{cases} \text{temperature} \\[6pt] \text{rod temperature (above the rod midpoint temperature datum)} \\[6pt] \text{temperature at distance } r \end{cases}$

t_∞ , the linear lateral temperature variation (above the rod midpoint temperature datum) in the solid at a radial distance sufficiently great so that the presence of the rod does not effect it

x , distance into the semi-infinite solid measured from the outer surface of the thin slab

z , distance along rod from rod midpoint

$\Delta t_{low\ k}$, the thermopile temperature difference for the low conductivity rod heat flux transducer

$\Delta t_{high\ k}$, the thermopile temperature difference for the high conductivity rod heat flux transducer

θ , time

ρ_∞ , density of the earth

XIV. APPENDIX

RECAPITULATION OF THE MATHEMATICAL MODELS FOR THE HEAT FLUX AND THERMAL CONDUCTIVITY TRANSDUCERS

A.   Rod Heat Flux Transducers

The temperature distribution along the rod heat flux transducer (see Figure 1) was described by,[3]

$$t = c_1 \left(e^{-\sqrt{C}z} - e^{\sqrt{C}z} \right) + \frac{B}{C} z$$

where

$$C = \frac{P}{R_\infty kA}$$

$$B = \frac{Pb}{R_\infty kA}$$

$$c_1 = \frac{-b}{-\sqrt{C} \left(e^{-\sqrt{C}\ell} + e^{\sqrt{C}\ell} \right) + \frac{1}{kR_e} \left(e^{-\sqrt{C}\ell} - e^{\sqrt{C}\ell} \right)}$$

$$R_\infty = \frac{r_i}{k_\infty} \ln \frac{r_o}{r_i}$$

$$R_e = \frac{r_i^2 \left(\frac{1}{r_i} - \frac{1}{r_o} \right)}{k_\infty}$$

When a transducer is used in a test hole, an annulus of either air or liquid surrounds the transducer. In order to account in the equations for the presence of this layer, the thermal resistance of the fluid annulus, R_{an}, is added to the cylindrical earth resistance to obtain an increased value for R_∞ (i.e., $R_\infty' = R_\infty + R_{an}$). Similarly, the effect of fluid at the ends of the transducer is also included, resulting in a modified R_e' (end heat conduction into a two region system). It is also noted that the end conduction term is relatively unimportant.

If the temperature solution for the high thermal conductivity rod transducer is divided by the temperature solution for the low thermal conductivity transducer, a single equation results which uniquely relates the earth thermal conductivity to the ratio of the thermopile voltages (temperature differences) and the radius r_o; this function for the Middletown transducers can be seen in Figure 2.

B. Thermal Conductivity Probe

The transient heat transfer performance of the thermal conductivity probe can be described by the classical step function surface heating boundary condition for a long cylinder (see Figure 3), namely,[4]

$$\frac{4\pi k_\infty}{2.30\,q}\, t = \int_{-\infty}^{\log \frac{k_\infty}{\rho_\infty c_{p\infty}}\theta} e^{-\frac{(r_o^2 + r^2)}{4\frac{k_\infty}{\rho_\infty c_{p\infty}}\theta}}\, J_o\left(\frac{i r_o r}{2\frac{k_\infty}{\rho_\infty c_{p\infty}}\theta}\right) d\left(\log \frac{k_\infty}{\rho_\infty c_{p\infty}}\theta\right)$$

The addition of a fluid annulus between the thermal conductivity probe and the borehole changes the conduction system into a two region problem. This boundary value problem was first solved by considering the annulus to be a thin slab located adjacent to a semi-infinite solid (the surrounding earth). The transient temperature solution for the annulus region is:[5]

$$t = \frac{(\frac{q}{A_0})\sqrt{D_1 D_2}}{\sqrt{D_1}k_2 + \sqrt{D_2}k_1} \sum_0^n \lambda^n \left[2\sqrt{\frac{\theta}{\pi}}\, e^{-\frac{(2an+x)^2}{4D_1\theta}} - \frac{(2an+x)}{\sqrt{D_1}}\, \mathrm{erfc}\left(\frac{2an+x}{2\sqrt{D_1\theta}}\right) \right.$$

$$\left. + 2\sqrt{\frac{\theta}{\pi}}\, e^{-\frac{(2an+2a-x)^2}{4D_1\theta}} - \frac{(2an+2a-x)}{\sqrt{D_1}}\, \mathrm{erfc}\left(\frac{2an+2a-x}{2\sqrt{D_1\theta}}\right) \right]$$

$$+ \frac{(\frac{q}{A_0})k_2}{\sqrt{D_1}k_2 + \sqrt{D_2}k_1}\left(\frac{D_1}{k_1}\right) \sum_0^n \lambda^n \left[2\sqrt{\frac{\theta}{\pi}}\, e^{-\frac{(2an+x)^2}{4D_1\theta}} - \frac{(2an+x)}{\sqrt{D_1}}\, \mathrm{erfc}\left(\frac{2an+x}{2\sqrt{D_1\theta}}\right) \right.$$

$$\left. - 2\sqrt{\frac{\theta}{\pi}}\, e^{-\frac{(2an+2a-x)^2}{4D_1\theta}} + \frac{(2an+2a-x)}{\sqrt{D_1}}\, \mathrm{erfc}\left(\frac{2an+2a-x}{2\sqrt{D_1\theta}}\right) \right]\, .$$

where $\quad \lambda = \dfrac{\sqrt{D_2}k_1 - \sqrt{D_1}k_2}{\sqrt{D_2}k_1 + \sqrt{D_1}k_2}$

and $n = 0, 1, 2 \ldots$

From the evaluation of this two-slab system it was shown that the temperature difference across the annulus is small in comparison to the transducer surface temperature rise above the initial temperature datum for times greater than the annulus time constant (which is of the order of 0.05 hours for a 0.2-inch thick water layer). Therefore, in the cylindrical coordinate system consisting of the fluid annulus and the surrounding semi-infinite earth, the annulus time constants and temperature drops will likewise be small compared to transducer values. It is felt that if the water annulus thickness is no more than 15 percent of the probe radius, then one can neglect the annulus effect (for times greater than the annulus time constant).

The calculated probe surface temperature rise versus time for typical earth thermal conductivity and specific heat per unit volume values is shown in Figure 4.[*] The thermal conductivity probe radius used is the same as that of the probe constructed by Geoscience and used at Middletown.

---

[*] From the generalized transient temperature solution for the thermal conductivity probe discussed previously,[4] one can simply plot specific time-temperature curves for a range of k_∞ and $\rho_\infty c_{p_\infty}$ values prior to a measurement effort; the curve which best fits the experimental time-temperature curve is readily identified.